

Intramolecular rearrangement of organosilyl groups between oxygen and nitrogen in aminosiloxanes – a joint experimental–theoretical study, part II

Susanne Kliem^a, Uwe Klingebiel^{a,*}, Mathias Noltemeyer^a, Stefan Schmatz^{*,b}

^a Institut für Anorganische Chemie der Georg-August-Universität Göttingen Tammannstr. 4, D-37077 Göttingen, Germany

^b Institut für Physikalische Chemie der Georg-August-Universität Göttingen, Tammannstr. 6, D-37077 Göttingen, Germany

Received 8 September 2004; accepted 6 October 2004

Abstract

Lithium amino-di-*tert*-butylsilanolate reacts with halosilanes to give 1-silylamino-1,3-siloxanes (**1–7**). The tetrakis(1-silylamino)siloxane thermally condenses yielding a spirocyclic six-membered ring (**8**). One six-membered ring of **8** forms a boat and the other has a twist conformation. Lithium salts of amino-disiloxanes form silylamino-silanolates or amido-disiloxanes. The first includes a 1,3-silyl group migration from the oxygen to the nitrogen atom. The energies of the isomeric lithium salts of model compounds are calculated and show that the lithium-trimethylsilylamino-dimethylsilanolate **III** is 0.7 kcal/mol more stable than the isomeric lithium-1,3-disiloxaneamide **V**. Experiments show that the lithium salts of amino-1,3-disiloxanes, (Me₃C)₂SiNH₂–O–R (R = SiMe₃, SiMe₂Ph, SiF₂CMe₃) reacts with ClSiMe₃, FSiMe₂Ph or F₃SiCMe₃ under a 1,3-O–N-silyl group migration to give the 1-silylamino-1,3-disiloxanes **9–11**. If the trimethylsilyl group is substituted by SiMeF₂, the difference between the isomers **III'** and **V'** is even smaller, 0.12 kcal/mol, and the barrier to reaction via the dyotropic transition state is calculated to be 10.1 kcal/mol. Interestingly, the fluorine atoms allow for two other isomers **VI** and **VIII** which are even lower in energy. The low difference in the energies of **III** and **V** respectively **VI** and **VIII** explains that in absence of steric and/or electronic restraints the lithium salts of amino-1,3-disiloxanes react halosilanes to give both isomeric silylamino-1,3-disiloxanes, e. g. the lithiated (Me₃C)₂SiNH₂–O–SiF₂CMe₃ reacts with F₂SiMe₂ or F₃SiPh to give the structural isomers **12**, **13**, and **14**, **15**.

The silyl group migration can be prevented kinetically, e. g. the lithium salts of (Me₃C)₂SiNH₂–O–R (R = SiF(N(CHMe₂)₂)₂, SiH(CMe₃)₂) react with F₂SiMe₂ or F₂Si(CMe₃)₂ to **16** and **17**. A thermodynamically prevented rearrangement is observed in the reaction of lithiated (Me₃C)₂SiNH₂–O–SiMe₃ with F₃SiR (R = CMe₃ (**18**), Ph (**19**), N(SiMe₃)₂ (**20**), C₆H₂ (CMe₃)₃ (**21**)). **18–21** ((Me₃C)₂SiNHSiF₂R)–O–SiMe₃) are formed.

LiF-elimination from (Me₃C)₂SiNHLiO–SiF₂Me leads to the formation of the eight-membered (SiOSiN)-ring **22**. The most stable lithium salts of 1-silylamino-1,3-disiloxanes form amides. This explains that in further reactions with halosilanes, the new ligand is bonded with the nitrogen atom (**28–30**). In results of crystal structure determinations new lithium-1-fluorosilylamino-1,3-disiloxanes of **20**, (**21**, **23–25**) are presented. **23** crystallizes as tricyclic, **24** as an unknown pentacyclic, and **25**, as monomeric compound. In **25** the shortest Si–N bond length (157.9 pm) with four coordinate silicon is found. Lithium salts of 1-fluorosilylamido-1,3-disiloxanes lose thermally LiF with formation of siloxane substituted cyclodisilazanes, **26** and **27**. Crystal structures of **4**, **8**, **17**, **20**, **21**, **22**, **23**, **24**, **25**, **26**, **28** are presented.

© 2004 Elsevier B.V. All rights reserved.

Keywords: Aminosiloxanes; Lithium salts; Isomerization; Quantum chemical calculations

* Corresponding author. Tel.: +49 551 393 052; fax: +49 551 393 373.

E-mail address: uklinge@gwdg.de (U. Klingebiel).

1. Introduction

Aminosilanes, silanols and aminosilanols can be stabilized kinetically by bulky groups, e.g. $(\text{Me}_3\text{C})_2\text{Si}(\text{OH})\text{NH}_2$ [1–12]. The lithium salt of this species was characterized as a tetramer, forming a Li–O cubane [1], while the sodium and potassium salts crystallize as hexagonal prisms [4]. The aminosilanolate reacts with halosilanes to give amino-1,3-siloxanes. In reactions of lithiated aminosiloxanes with halosilanes often a 1,3-silyl group migration from oxygen to the nitrogen is observed. 1-Silyl-amino-1,3-disiloxanes are formed. However, 1,3-silyl group migration does not occur in reactions of lithiated 1-silylamino-1,3-disiloxanes [1].

In this work, we present our experimental results – especially X-ray crystal structure determinations of unusual lithium salts of 1-fluorosilyl-1,3-disiloxanes – and rationalize them by means of quantum-chemical calculations. All theoretical results given in this work are obtained from density functional calculations employing the variant B3LYP and the large 6-311+G(2d,p) basis set (see Section 3.9 for further details).

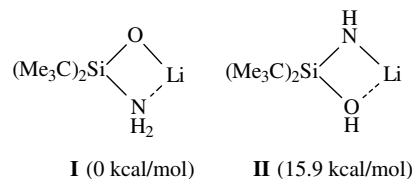
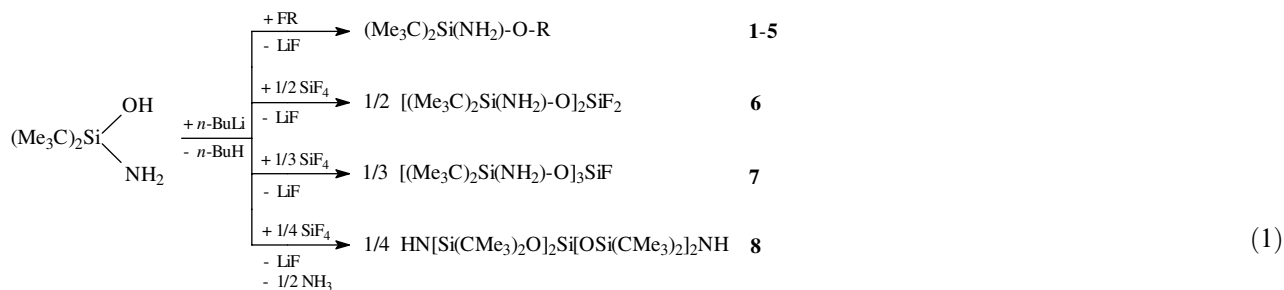


Fig. 1. Relative energies of isomeric lithium salts **I** and **II**.

(159.5 pm), whereas the Si–N bond distance amounts to 184.1 pm. The Si–O–Li angle is obtained to be 94.1° and the Si–N–Li angle measures 77.3° .

The less stable isomer $\text{Me}_2\text{Si}(\text{OH})\text{NHLi}$ (**II**) has two almost similar O–Li (189.5 pm) and N–Li (181.3 pm) distances. As expected, the Si–N bond (167.2 pm) is shortened and the Si–O distance (175.0 pm) has become longer. The Si–N–Li angle (92.1°) has considerably increased while the Si–O–Li angle (87.0°) is only slightly smaller than in **I**.

The stability of the alkaline amino-silanolate explains the position of substituents. E.g. in reactions with halosilanes, numerous mono-, bis-, tris- and tetrakis-1-amino-siloxanes are formed [1–4].



	1	2	3	4	5
R	SiH(CMe ₃) ₂	SiFMePh	SiF ₂ Ph	SiF ₂ C(SiMe ₃) ₃	2,2,6,6-Tetramethylpiperidine

The unstable tetrakis-(1-amino-siloxane) condenses thermally yielding a spirocyclic six-membered ring (**8**) and NH₃.

2. Results and discussion

2.1. 1-Aminosiloxanes

The aminosilanolate anion **I** is 15.9 kcal/mol more stable than the isoelectronic amidosilanolate anion **II** (see Fig. 1).

Both isomers form four-membered ring systems where the lithium is bonded both to the nitrogen and oxygen atoms. In the $\text{Me}_2\text{Si}(\text{NH}_2)\text{OLi}$ species **I**, the lithium is closely bound to the oxygen atom ($r(\text{O-Li}) = 173.8$ pm), while the contact to the nitrogen is as large as 206.0 pm. The Si–O bond is relatively short

The unstable tetrakis-(1-amino-siloxane) condenses thermally yielding a spirocyclic six-membered ring (**8**) and NH₃.

*Crystal structure of $(\text{Me}_3\text{C})_2\text{Si}(\text{NH}_2)\text{-O-SiF}_2\text{C}(\text{SiMe}_3)_3$ (**4**).* Compound **4** (Fig. 2, Table 1) crystallizes from *n*-hexane in the space group $P(2)1/n$. Due to the electron withdrawing effect of the fluorine atoms, the Si(1)–O(1) bond length is 7.2 pm shorter than the Si(2)–O(1) bond.

*Crystal structure of $\text{HN}[\text{Si}(\text{CMe}_3)_2\text{O}]_2\text{Si}[\text{OSi}(\text{CMe}_3)_2]_2\text{NH}$ (**8**).* Crystals of **8** were obtained from *n*-hexane, space group $P(2)1/c$. This spirocyclic compound has some interesting structural features. One six-membered

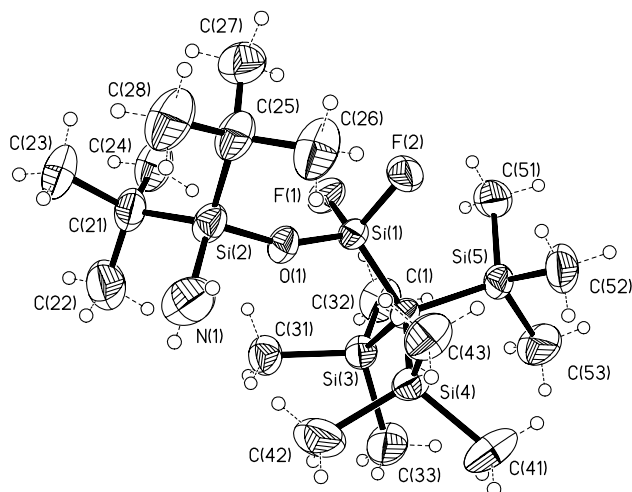
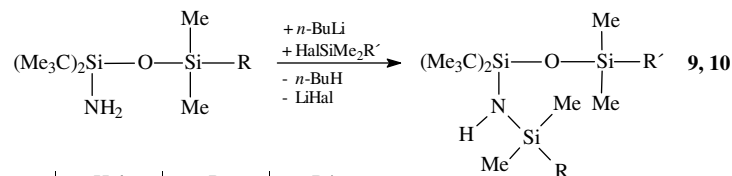


Fig. 2. Structure of **4**; selected bond lengths (pm) and angles ($^{\circ}$): Si(1)–F(2) 158.6(2), Si(1)–F(1) 159.1(2), Si(1)–O(1) 159.1(2), Si(1)–C(1) 183.2(2), Si(2)–O(1) 166.3(2), Si(2)–N(1) 169.9(3), C(1)–Si(5) 193.2(2), Si(5)–C(51) 189.3(3); F(2)–Si(1)–F(1) 102.6(9), F(2)–Si(1)–O(1) 107.5(9), F(1)–Si(1)–O(1) 106.9(9), F(2)–Si(1)–C(1) 110.4(9), O(1)–Si(2)–N(1) 108.5(1), O(1)–Si(1)–C(1) 118.1(1), Si(1)–O(1)–Si(2) 159.7(1), Si(4)–C(1)–Si(5) 109.9(1).

ring forms a boat and the other one has a twisted conformation. Some of the Si–N bonds are shorter than the Si–O bonds (see Fig. 3).



	Hal	R	R'
9	Cl	Ph	Me
10	F	Me	Ph

2.2. 1-Silylamino-1,3-disiloxanes

2.2.1. 1,3-(O → N)-silyl group migration

Substitutions of the 1-amino-siloxanes turn out to be more complicated. Lithium salts of these compounds form, depending on the properties and bulkiness of the silyl groups, 1,3-disilylamino-1-olates or the less stable 1-amido-1,3-disiloxanes. The second case includes a 1,3-silyl group migration from the oxygen to the nitrogen atom.

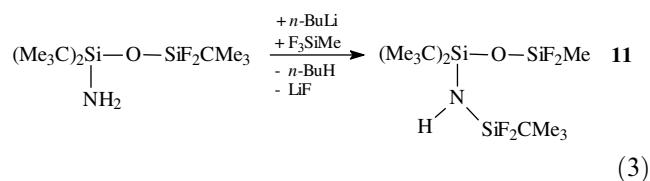
In order to understand the driving force of this isomerisation, we have calculated the energies of the isomeric lithium salts of the model compound $\text{Me}_2\text{Si}(\text{NH}_2)\text{O}-\text{SiMe}_3$ and found that the lithium-silylamino-silanolate (**III**) is only 0.7 kcal/mol more stable than the isomeric lithium-1,3-disiloxaneamide (**V**) (see Fig. 4).

When one of the hydrogen atoms at OH/NH₂ is replaced by a trimethylsilyl group, different isomers are

possible. In particular, the amide species is only 0.7 kcal/mol higher in energy than the olate species. The isomerisation between the two isomers, i.e. the migration of the trimethylsilyl group passes a dyotropic transition state (see Fig. 5) that is relatively similar to the cases investigated so far [10–15]. The O–N unit is bridged by two silicon atoms. However, here we have the additional bridging lithium cation so that the structure is somewhat more complex. The Si–Si distance amounts to 269.1 pm and the distance between the oxygen and nitrogen atoms, respectively, and the silicon atom are as follows: $r(\text{Me}_3\text{Si}-\text{O}) = 185.9$ pm, $r(\text{O}-\text{SiMe}_2) = 167.2$ pm, $r(\text{Me}_3\text{Si}-\text{N}) = 208.9$ pm, $r(\text{N}-\text{SiMe}_2) = 172.3$ pm. The distance of the lithium to the nitrogen atom amounts to 196.1 pm and that to the oxygen atom is calculated to be 203.8 pm. The angle Si–O–Si is obtained to be 99.2° , while the Si–N–Si angle is somewhat smaller (89.3°). The vibrational frequency of the transition mode amounts to 155 i cm^{-1} .

The experimental results are in good agreement with the quantum chemical calculations. In the reaction of the lithium salts of the amino-1,3-disiloxanes, $(\text{Me}_3\text{C})_2\text{Si}(\text{NH}_2)\text{O}-\text{SiMe}_2\text{R}$ with Me_3SiCl or PhMe_2SiF the 1-silylamino-1,3-disiloxanes (**9**, **10**) are formed under a 1,3-O → N-silyl group migration.

Comparable rearrangements are obtained using fluoro-silylsubstituted amino-1,3-disiloxanes, e.g. in reactions of the lithium salt of $(\text{Me}_3\text{C})_2\text{Si}(\text{NH}_2)\text{O}-\text{SiF}_2\text{CMe}_3$ with F_3SiMe . The F_2SiCMe_3 group migrates from the oxygen to the nitrogen atom.



Quantum chemical calculations of the lithiated model compound $\text{Me}_2\text{Si}(\text{NH}_2)\text{O}-\text{SiF}_2\text{Me}$ confirm the experimental results, the olate isomer (**VI**) is 6.4 kcal/mol more stable than the amide isomer (**VIII**) which can be formed via the transition state **VII** (see Fig. 6).

Table 1

Compound	4	8	17	20
Identification code	uwe187	uwe168x	Uwe202	uwe169a
Empirical formula	C ₁₈ H ₄₇ F ₂ NOSi ₅	C ₃₂ H ₇₄ N ₂ O ₄ Si ₅	C ₂₄ H ₅₆ FNOSi ₃	C ₁₇ H ₄₅ F ₂ N ₂ OSi ₅
Formula weight	472.02	691.38	477.97	472.00
<i>T</i> (K)	203(2)	293(2)	203(2)	250(2)
λ (pm)	71.073	71.073	71.073	71.073
Crystal system	Monoclinic	Monoclinic	Monoclinic	Monoclinic
Space group	<i>P2(1)/n</i>	<i>P2(1)/c</i>	<i>P2(1)/n</i>	<i>P2(1)/c</i>
Unit cell dimensions				
<i>a</i> (pm)	1267.2(3)	1228.8(3)	1631.7(3)	1189.4(2)
<i>b</i> (pm)	1482.9(4)	1630.3(3)	1181.5(2)	1441.5(3)
<i>c</i> (pm)	1609.0(4)	2231.0(5)	1738.5(4)	1816.1(4)
α (°)	90	90	90	90
β (°)	112.788(19)	105.53(3)	114.80(3)	108.49(3)
γ (°)	90	90	90	90
<i>V</i> (nm ³)	2.7875(12)	4.3061(15)	3.0423(11)	2.9532(10)
<i>Z</i>	4	4	4	4
<i>D</i> _{calc} (Mg/m ³)	1.125	1.066	1.044	1.062
Absorption coefficient (mm ⁻¹)	0.279	0.198	0.177	0.264
<i>F</i> (000)	1032	1528	1064	1028
Crystal size (mm ³)	1.00 × 0.70 × 0.60	0.80 × 0.800 × 0.40	0.80 × 0.70 × 0.60	1.00 × 1.00 × 0.30
θ Range for data collection (°)	3.51–25.06	3.54–22.49	3.52–25.02	3.61–22.51
Index ranges	–15 ≤ <i>h</i> ≤ 15, –10 ≤ <i>k</i> ≤ 17, –16 ≤ <i>l</i> ≤ 19	–13 ≤ <i>h</i> ≤ 13, –17 ≤ <i>k</i> ≤ 17, –8 ≤ <i>l</i> ≤ 23	–19 ≤ <i>h</i> ≤ 19, –11 ≤ <i>k</i> ≤ 14, –20 ≤ <i>l</i> ≤ 20	–12 ≤ <i>h</i> ≤ 12, –15 ≤ <i>k</i> ≤ 15, –19 ≤ <i>l</i> ≤ 19
Reflections collected	5220	3396	6260	11036
Independent reflections (<i>R</i> _{int})	4922 (0.0464)	2951 (0.0941)	5339 (0.0997)	3846 (0.0758)
Completeness	to $\theta = 25.06^\circ$, 99.5%	to $\theta = 22.49^\circ$, 52.5%	to $\theta = 25.02^\circ$, 99.6%	to $\theta = 22.51^\circ$, 99.5%
Maximum and minimum transmission	0.9835 and 0.7681		0.9013 and 0.8715	0.9250 and 0.7783
Refinement method	Full-matrix least-squares on <i>F</i> ²	Full-matrix least-squares on <i>F</i> ²	Full-matrix least-squares on <i>F</i> ²	Full-matrix least-squares on <i>F</i> ²
Data/restraints/parameters	4922/4/284	2951/575/397	5339/406/298	3846/145/259
Goodness-of-fit on <i>F</i> ²	1.086	1.062	1.019	1.067
Final <i>R</i> indices [<i>I</i> > 2 σ (<i>I</i>)]	<i>R</i> ₁ = 0.0563, <i>wR</i> ₂ = 0.1545	<i>R</i> ₁ = 0.0956, <i>wR</i> ₂ = 0.2091	<i>R</i> ₁ = 0.0724, <i>wR</i> ₂ = 0.2087	<i>R</i> ₁ = 0.0678, <i>wR</i> ₂ = 0.1914
<i>R</i> indices (all data)	<i>R</i> ₁ = 0.0623, <i>wR</i> ₂ = 0.1624	<i>R</i> ₁ = 0.1390, <i>wR</i> ₂ = 0.2391	<i>R</i> ₁ = 0.0810, <i>wR</i> ₂ = 0.2216	<i>R</i> ₁ = 0.0802, <i>wR</i> ₂ = 0.2070
Largest difference peak and hole (e Å ⁻³)	0.456 and –0.397	0.355 and –0.367	1.251 and –0.612	0.452 and –0.309

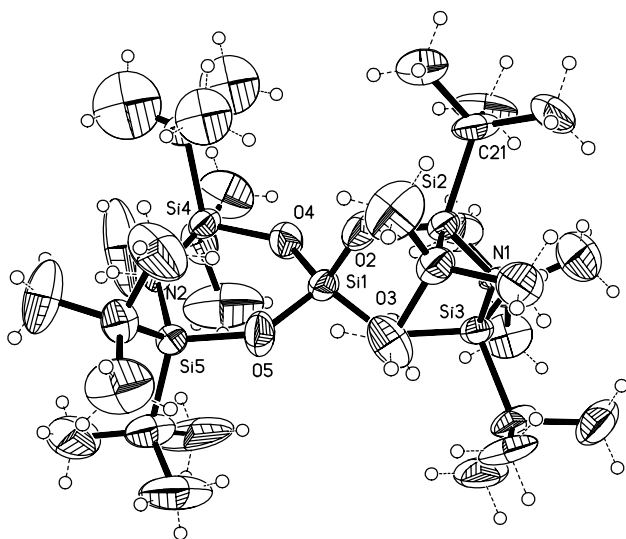


Fig. 3. Structure of **8**; selected bond lengths (pm) and angles ($^{\circ}$): Si(1)–O(4) 163.6(7), Si(1)–O(2) 162.3(6), Si(1)–O(5) 164.7(1), Si(1)–O(3) 166.9(1), N(1)–Si(3) 166.2(6), Si(2)–O(2) 165.7(8), N(2)–Si(4) 164.8(1), Si(3)–O(3) 169.6(1); O(2)–Si(1)–O(3) 106.5(5), O(4)–Si(1)–O(3) 112.0(5), Si(3)–N(1)–Si(2) 134.3(6), Si(4)–N(2)–Si(5) 135.8(6), Si(1)–O(2)–Si(2) 134.2(5), Si(1)–O(3)–Si(3) 132.1(5), O(5)–Si(5)–N(2) 103.4(6), Si(1)–O(5)–Si(5) 135.0(5).

When the trimethylsilyl group is substituted by Si-MeF₂, the difference between the isomers **VI'** and **VIII'** is even smaller, 0.12 kcal/mol, and the barrier to reaction

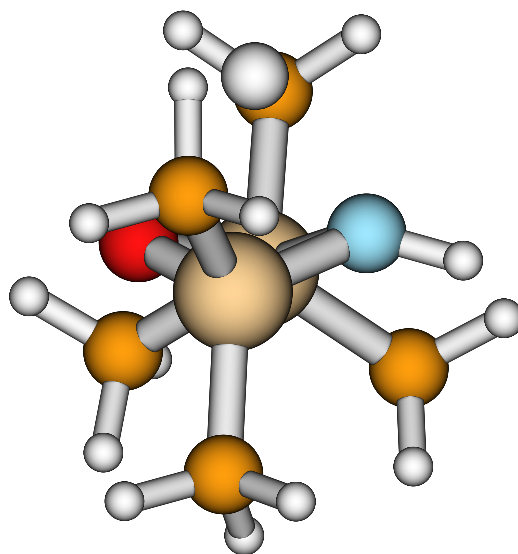


Fig. 5. Calculated [B3LYP/6-311+G(2d,p)] structure of transition state **IV**.

via the dyotropic transition state is calculated to be 10.1 kcal/mol (see Fig. 6). Interestingly, the fluorine atoms allow for two other isomers **VI** and **VIII** which are even lower in energy. The fluorine is able to coordinate the lithium and two stable six-membered rings are possible. The olate species is 6.4 kcal/mol lower in energy than the amide species.

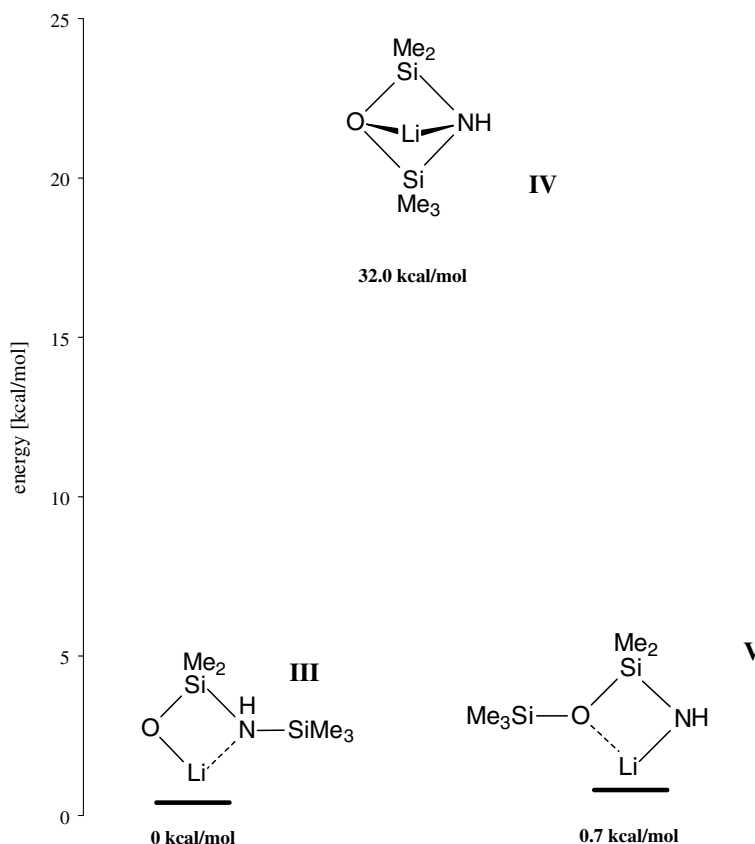


Fig. 4. Relative energies of the isomeric lithium salts **III** and **V**, and the saddle point structure ('transition state') corresponding to isomerization (**IV**).

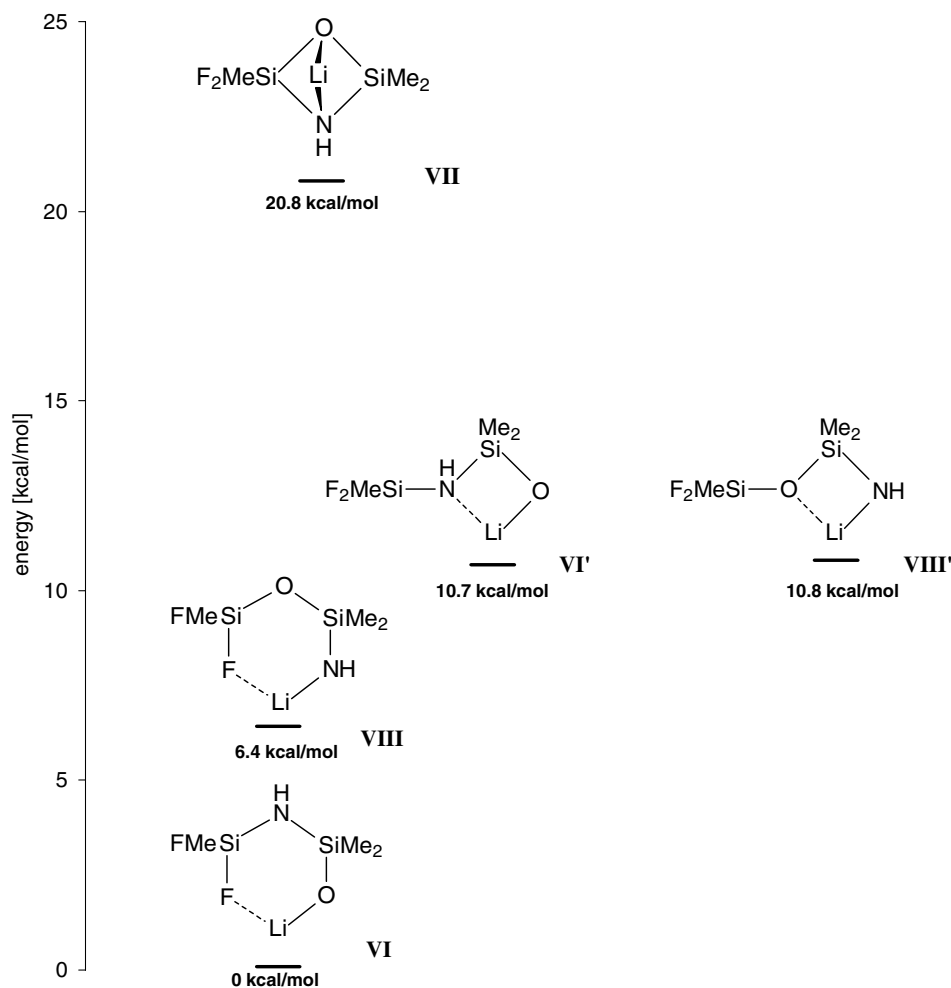
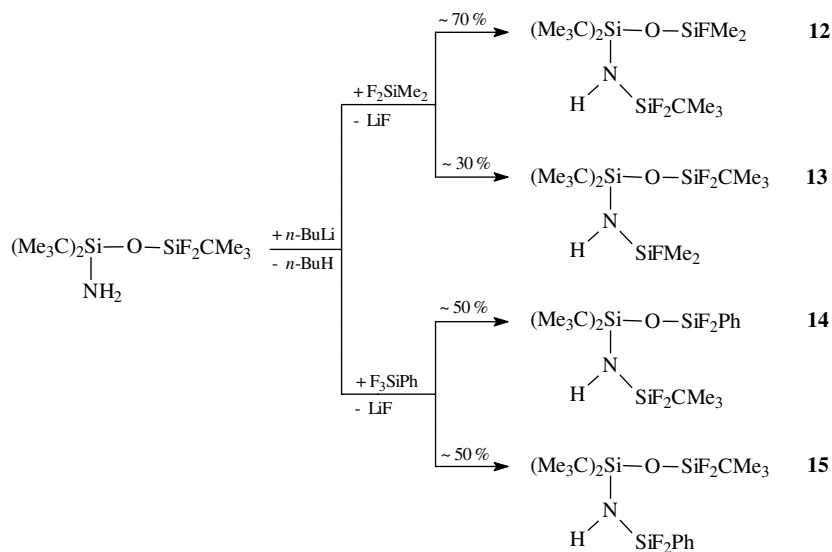


Fig. 6. Relative energies of isomeric lithium salts VI–VIII.

The low difference in the energies between III and V as well as VI and VIII explains that in the absence of steric and/or electronic restraints the

lithium salts of amino-1,3-disiloxanes react with halo-silanes to give both isomeric silylamino-1,3-disiloxanes, e.g.



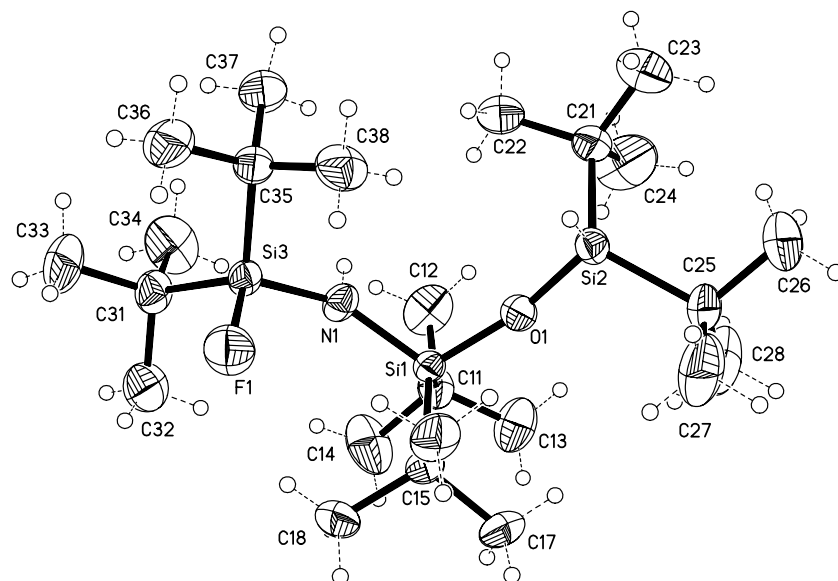
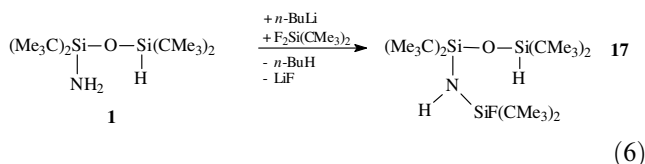
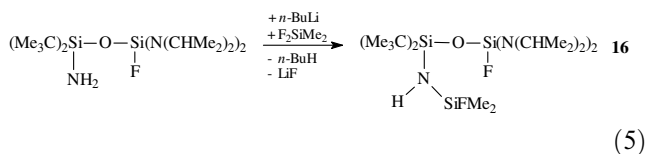


Fig. 7. Structure of **17**; selected bond lengths (pm) and angles ($^{\circ}$): Si(1)–O(1) 165.0(2), Si(1)–N(1) 171.5(2), Si(2)–O(1) 161.8(2), Si(3)–F(1) 158.2(2), Si(3)–N(1) 170.8(2); Si(3)–N(1)–Si(1) 148.2(2), Si(2)–O(1)–Si(1) 164.1(2), O(1)–Si(1)–N(1) 110.8(1), C(21)–Si(2)–C(25) 116.0(2), F(1)–Si(3)–N(1) 107.8(1).

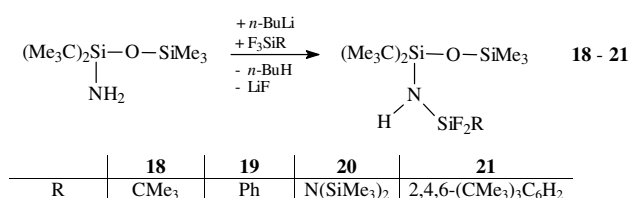
2.2.2. Retention of the siloxane unit

2.2.2.1. *Kinetically prevented rearrangement.* Bulky groups prevent kinetically the silyl group migration from the oxygen to the nitrogen atom, e.g.



Crystal structure of $(\text{Me}_3\text{C})_2\text{Si}[\text{NHSiF}(\text{CMe}_3)_2]-\text{O}-\text{SiH}(\text{CMe}_3)_2$, (**17**). Crystals of **17** were obtained from *n*-hexane with the space group $P2(1)/n$. The angles at the oxygen and nitrogen atoms are unusually widened. The Si(1)–N(1)–Si(3) angle is measured with 148.2° and the Si(1)–O(1)–Si(2) angle with 164.1° (see Fig. 7).

2.2.2.2. *Thermodynamically prevented rearrangement.* Starting with lithium salts of 1-amino-1.1.3.3.3-pentaorganyl-1,3-disiloxanes, reactions with trifluorosilanes lead only to 1-difluorosilylamino-1,3-disiloxanes.



The formation of these *N*-difluorosilylamino-1,3-disiloxanes promoted us to study the relative energies of model compounds **IX** and **X** (see Fig. 8).

We found that **IX** is 0.8 kcal/mol more stable than **X**. Though this is not very much, we could not isolate isomeric compounds of **18–21**.

Crystal structures of $(\text{Me}_3\text{C})_2\text{Si}[\text{NHSiF}_2\text{N}(\text{SiMe}_3)_2]-\text{O}-\text{SiMe}_3$ (**20**) and $(\text{Me}_3\text{C})_2\text{Si}[\text{NHSiF}_2-2,4,6(\text{CMe}_3)_3\text{C}_6\text{H}_2]-\text{O}-\text{SiMe}_3$ (**21**). The retention of the siloxane unit in the reaction of 1-amino-1,3-disiloxanes with *n*-BuLi and trifluorosilanes could be proved by X-ray crystallography of compounds **20** and **21**. Compounds **20** and **21** crystallize from *n*-hexane as monomers in the monoclinic crystal system space group $P2(1)/c$ (**20**), $P2(1)/n$ (**21**). In both compounds N–H or F–H donor bonds do not exist. Steric effects may be the reason for the wide angle at the oxygen atom. Because of the electron withdrawing effect of the fluorine atoms, the Si–N bond lengths in neighborhood to SiF₂ group are shorter than the others. The N-atoms have a planar environment. The bulky groups at the siloxane unit are the reason for the large Si–O–Si angle (172.37° (**20**), 177.17° (**21**)) (see Figs. 9 and 10)

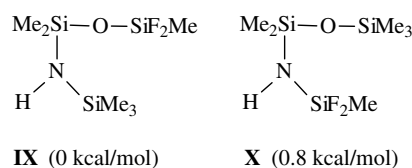


Fig. 8. Relative energies of isomeric lithium salts **IX**, **X**.

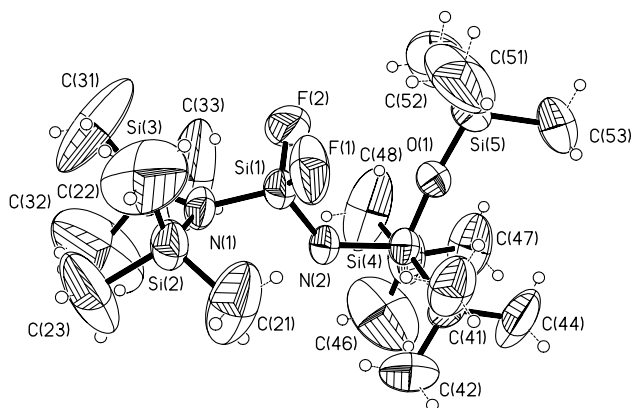
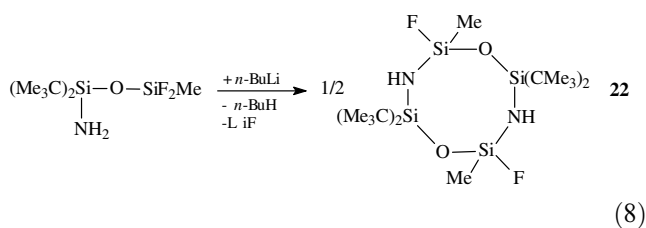


Fig. 9. Structure of **20**; selected bond lengths (pm) and angles ($^{\circ}$): Si(1)–F(2) 156.3(1), Si(1)–N(2) 166.6(1), Si(1)–N(1) 169.2(1), N(2)–Si(4) 174.0(1), N(1)–Si(2) 175.0(1), O(1)–Si(4) 159.6(9), O(1)–Si(5) 161.6(1); F(2)–Si(1)–F(1) 102.1(7), N(1)–Si(1)–N(2) 114.6(6), Si(1)–N(1)–Si(3) 119.7(6), Si(4)–O(1)–Si(5) 172.4(5), O(1)–Si(4)–N(2) 107.0(4), Si(1)–N(1)–Si(2) 118.2(6), Si(3)–N(1)–Si(2) 121.9(5).

2.3. (SiOSiNH)-rings

Experimental results show that LiF-elimination from lithiated 1-fluoro-1,3-disilazane-1-olates (**VI**) leads to the formation of four- or eight-membered (SiOSiN)₂-rings [1], e.g.



Crystal structure of [(Me₃C)₂SiNHSiFMeO]₂ (**22**). The structure determinations of known (Si–O–Si–NH)₂-eight-membered rings and also of **22** show most effectively planar rings. Such backbones in molecular structures are rare. Particularly unusual features of these compounds are the virtually linear Si–O–Si (174.3 $^{\circ}$) units in the ring. The Si–O and Si–N bond lengths are remarkable, they are within the same range, Si(1)–O(1) = 160.1 pm, Si(1)–N(1) = 166.1 pm, Si(2)–O(1) = 159.6 pm, Si(2)–N(1A) = 160.7 pm. LiF-elimination from lithium salts of bulky substituted 1-fluorosilylamino-1,3-disiloxanes lead to the formation of four-membered (SiOSiNH)-rings (Fig. 11).

2.4. Lithium-1-silylamido-1,3-disiloxanes

2.4.1. Quantum chemical calculations

In contrast to lithium salts of aminosilanols and aminosiloxanes, quantum chemical calculations for model compounds like lithiated silylamino-1,3-disiloxanes show that in this case the most stable salt is the model 1-silylamido-1,3-disiloxane (**XI**), which is 19.2

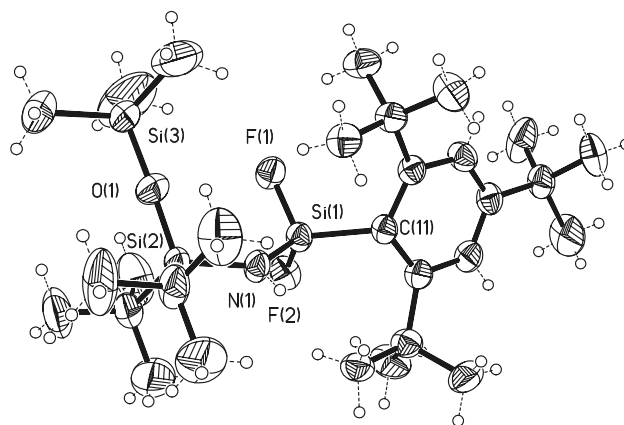


Fig. 10. Structure of **21**; selected bond lengths (pm) and angles ($^{\circ}$): Si(1)–F(1) 158.6(2), Si(1)–F(2) 158.7(2), Si(1)–N(1) 168.5(2), Si(1)–C(11) 186.5(3), O(1)–Si(2) 160.6(2), N(1)–Si(2) 173.4(2); Si(1)–N(1)–Si(2) 135.8(2), Si(2)–O(1)–Si(3) 177.2(2), F(2)–Si(1)–F(1) 100.4(1), F(1)–Si(1)–N(1) 107.0(1), F(1)–Si(1)–C(11) 108.7(1), N(1)–Si(1)–C(11) 122.7(1).

kcal/mol more stable than the possible model olate isomer **XII** (see Fig. 12).

In the compound Me₂Si(OSiMe₃)N(SiMe₃)Li, again a four-membered ring (**XI**) is formed with contacts from the lithium atom to both nitrogen (184.1 pm) and oxygen (190.4 pm). The ring exhibits C_s symmetry. After migration of one trimethylsilyl group from the oxygen to the nitrogen atom, the olate structure is recovered which is 19.2 kcal/mol higher in energy than the amide structure. The N atom in **XII** has an almost planar surrounding with a Li–N contact of 216.5 pm. The Li–N contact in **XI** is calculated to be only 184.1 pm.

In lithium salts of fluoro containing 1-silylamino-1,3-disiloxane, the hard Lewis acid lithium additionally binds the hard Lewis base fluorine. Again, the silyl group migration affords too much energy, so that the new ligand will be bonded to the nitrogen atom (see Fig. 13).

We have now combined the two substitutions of our last two series of calculations: The two hydrogen atoms are now substituted by a SiMe₃ and a SiMeF₂ group (see Fig. 14). Here, we find isomers not encountered before. The most stable structure **XIII** is of amide-type and is characterized as a bicyclus formed by two four-membered rings where the lithium cation has close contacts to the oxygen atom, the nitrogen atom and one of the fluorine atoms (see Fig. 14).

10.2 kcal/mol higher in energy is a similar structure where the close proximity of the lithium cation to the nitrogen atom is lost and contacts to both fluorine atoms of the SiMeF₂ group are formed (**XVI**).

The corresponding isomer with contacts of the lithium cation to oxygen and nitrogen only, i.e. with the SiMeF₂ group turned away from the lithium atom, could again not be converged in our B3LYP calculations with the large 6-311+G(2d,p) basis set. The molecules always attained the global minimum structure (**XIII**). Only with

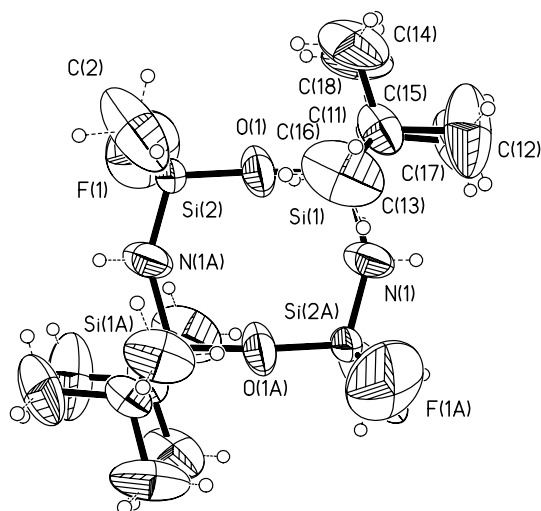


Fig. 11. Structure of **22**; selected bond lengths (pm) and angles ($^{\circ}$): Si(2)–O(1) 159.6(4), Si(1)–O(1) 160.1(4), Si(1)–N(1) 166.1(5), Si(2)–N(1A) 160.7(4), Si(1)–C(15) 188.7(5), Si(2)–F(1) 165.9(6), Si(2)–C(2) 173.3(7); O(1)–Si(1)–N(1) 106.0(3), O(1)–Si(1)–C(11) 109.7(3), O(1)–Si(2)–N(1A) 108.2(3), O(1)–Si(2)–F(1) 109.1(4), Si(2)–O(1)–Si(1) 175.3(4), Si(2A)–N(1)–Si(1) 149.5(4).

the smaller basis set 6-31G(d) we obtained the result that this structure (**XV**) is 7.1 kcal/mol above the most stable isomer.

Another possible amide-type structure is obtained after exchange of the SiMe₃ and SiMeF₂ groups at oxygen and nitrogen, respectively. Here, a six-membered ring **XIV** is formed with lithium contacts to fluorine

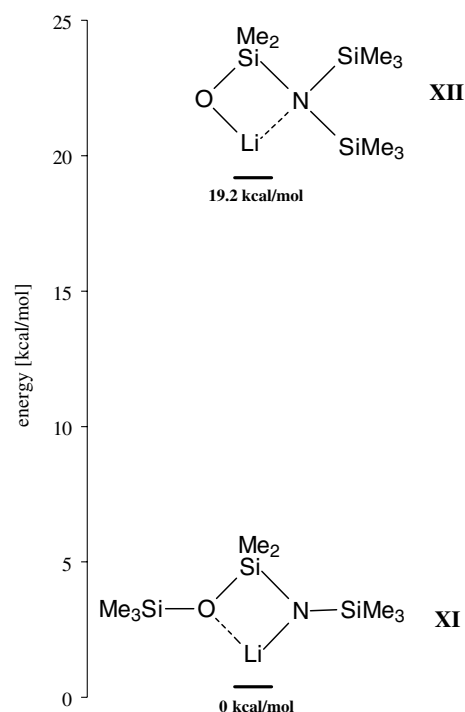


Fig. 12. Relative energies of isomeric lithium salts **XI**, **XII**.

and nitrogen. In contrast to isomer **XIII**, no transannular contact to the oxygen atom is possible because the negative charge is mainly located at the nitrogen and not at the oxygen site.

The isomer that is highest in energy is the olate structure **XVII** which again forms a six-membered ring with

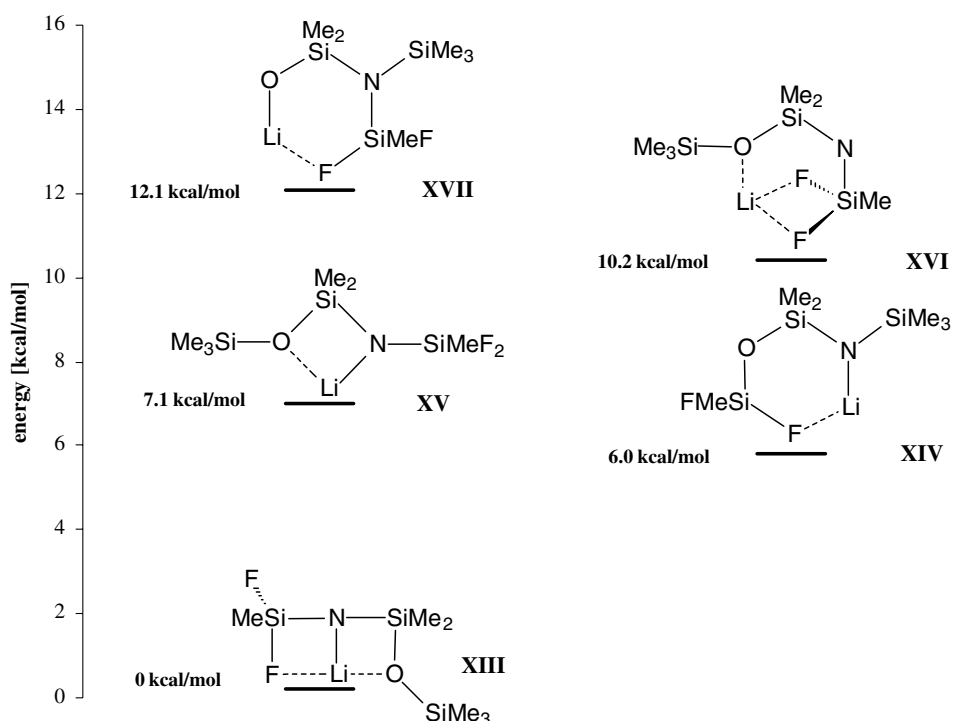


Fig. 13. Relative energies of isomeric lithium salts **XIII**–**XVII**.

contacts of the lithium cation to the oxygen and one of the fluorine atoms.

The stability of the lithium-silyl-amides **XIII**–**XVI** explains that in further reactions with halosilanes the new ligand will be bonded at the nitrogen site.

2.4.2. Synthesis and crystal structures

In chemical experiments, lithium salts of type **XV** and **XVI** could be isolated as dimers. **XV** forms a tricyclic compound existing as two (SiOSiN)-four-membered rings connected by a (LiFSiN)₂-eight-membered ring and **XVI** forms a spiro-pentacyclic compound existing as two (SiOSiN)-four-membered rings and two (Si-F₂Li)-four-membered rings which are connected by a (LiNSiF₂)₂-eight-membered ring system.

The lithium compound **23** is obtained in high yields from the reaction of **20** with *n*-BuLi, thus forming structure **23**.

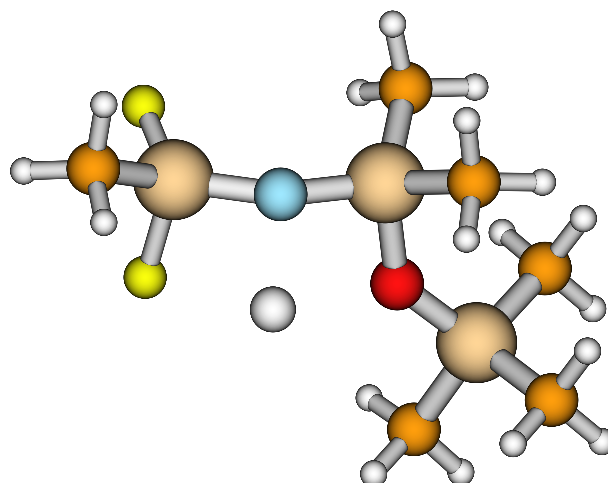
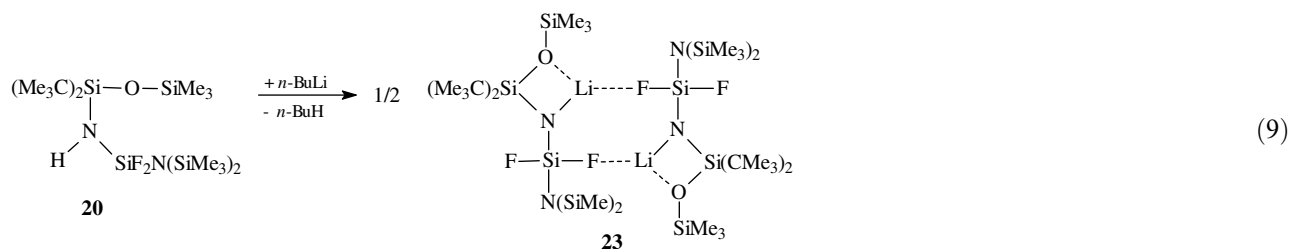


Fig. 14. Calculated [B3LYP/6-311+G(2d,p)] structure of **XIII**.

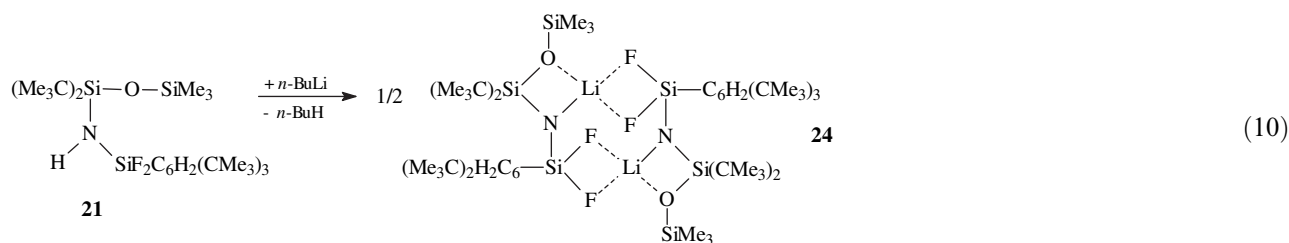


*Crystal structure of (Me₃Si)₂N-SiF₂-NLi-Si(CMe₃)₂-O-SiMe₃ (**23**).* Compound **23** crystallizes from *n*-hexane as a dimer in the space group *P2*(1)/*c*. The crystal structure of **23** shows some irregularities: One Si–F bond length is, because of the Li–F contact, 5.3 pm longer than the other. The Si(1)–N(1) bond length is in the range of a double bond length. The Li–O contact lengthens the Si(2)–O(1) bond. The Li–F contact (181.8 pm) is unusually short even shorter than the Li–N bond (193.2 pm). Lithium is only three coordinated ($\sum^\circ \text{Li} = 349.7^\circ$) (see Fig. 15).

*Synthesis and crystal structures of lithiated 2,4,6-(Me₃C)₃C₆H₂-SiF₂NHSi(CMe₃)₂-O-SiMe₃ (**24**, **25**).* The lithium salt **24** is obtained in the reaction of **21** and *n*-BuLi, thus forming the pentacyclus **24**.

Compound **24** crystallizes from *n*-hexane as a dimer in the space group *P1* (see Fig. 16).

The lithium atom has a tetrahedral coordination (two fluorine, one oxygen and one amido contact) and forms a spirocyclohexane with two four-membered rings, an (OSiN-Li)- and an (FSiFLi)-ring. The two spirocyclic units of the dimer are connected by an eight-membered (NSiFLi)₂-ring. A pentacyclus is formed. Because of the electron withdrawing effect of the fluorine atoms the Si(1)–N(1) bond length is shortened, the Si(1)–N(1)–Si(2) (167.6°) is widened. The nitrogen atom has a planar environment. The ion F(1A)–Li(1)–F(2A) angle at the tetrahedral lithium amounts to only 69.6°. A quartet ($J_{\text{FLi}} = 57.1$ Hz) is found in the ¹⁹F nmr spectrum and a triplet in the ⁷Li-nmr spectrum. This indicates that the



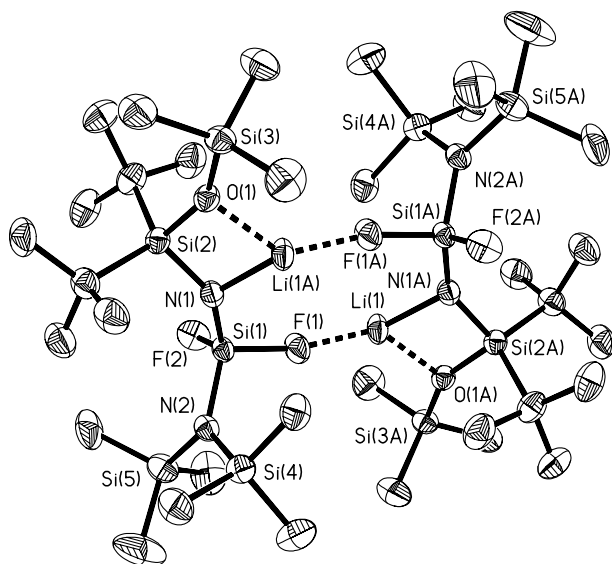


Fig. 15. Structure of **23**; selected bond lengths (pm) and angles ($^{\circ}$): Si(1)–F(2) 159.3(2), Si(1)–F(1) 164.7(3), Si(1)–N(1) 160.9(3), Si(1)–N(2) 171.1(3), Si(2)–N(1) 167.2(3), Si(2)–O(1) 168.7(3), Si(3)–O(1) 164.3(3), Li(1)–F(1) 181.8(8), Li(1)–N(1A) 193.2(8), Li(1)–O(1A) 200.0(7), Si(3)–O(1)–Si(2) 153.0(2), Si(3)–O(1)–Li(1A) 119.6(3), Si(2)–O(1)–Li(1A) 87.4(2), Si(1)–N(1)–Si(2) 145.8(2), Si(1)–F(1)–Li(1) 165.6(2), Si(1)–N(1)–Li(1A) 123.9(3), Si(2)–N(1)–Li(1A) 90.1(2), F(1)–Li(1)–O(1A) 131.4(4), N(1A)–Li(1)–O(1A) 82.0(3), F(1)–Li(1)–Si(2A) 154.3(4).

dimer exists in an unpolar solution (*n*-hexane, C_6D_6), too.

Crystallization of **24** from thf leads to a complete rupture of the Li–N contact. The monomeric lithium salt **25** is formed (see Fig. 17).

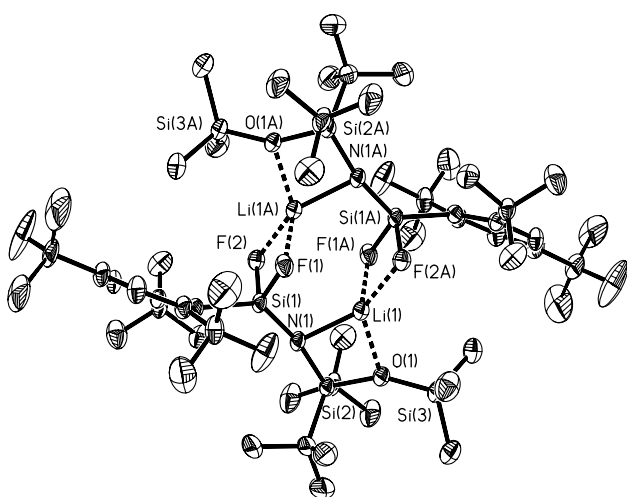
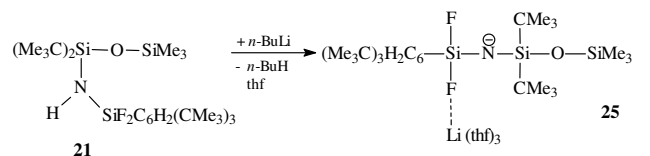


Fig. 16. Structure of **24**; selected bond lengths (pm) and angles ($^{\circ}$): Si(1)–N(1) 160.7(3), Si(1)–F(1) 164.8(2), Si(1)–Li(1A) 282.8(6), F(1)–Li(1A) 200.6(6), O(1)–Si(2) 168.7(3), N(1)–Li(1) 204.5(6), Li(1)–Si(2) 260.2(6), F(2)–Si(1)–F(1) 89.1(1), N(1)–Si(1)–C(11) 132.6(1), Si(1)–F(1)–Li(1A) 101.0(2), Si(3)–O(1)–Si(2) 153.6(2), Si(1)–N(1)–Si(2) 167.6(2), Si(1)–N(1)–Li(1) 104.0(2), F(1A)–Li(1)–F(2A) 69.6(2).



(11)

Lithium now has migrated to the stronger Lewis base fluorine. The result is a short Li–F bond (186.6 pm) and two different Si–F bond lengths, a short one, Si(1)–F(2) = 162.0 pm, and a long one, Si(1)–F(1) = 165.9 pm. The Si–N bond has a double bond length of 157.9 pm. As far as we know, this is the shortest Si–N bond with four coordinated silicons. The Si–N–Si angle of 167.2° is typical of an imine. Therefore, the molecule must be considered as an Li–F adduct of an iminosilane, as demonstrated in Fig. 18.

The ^{19}F -nmr and ^{29}Si -nmr spectra show equivalent fluorine atoms. This indicates a fluctuation of the lithium ion in solution.

2.5. Reactions of Lithium-1-fluorosilylamido-1,3-disiloxanes

2.5.1. Formation of cyclosilazanes

Lithium salts of 1-fluorosilylamido-1,3-disiloxanes of type **XIII** lose thermally LiF under formation of siloxane substituted cyclodisilazanes, e.g.

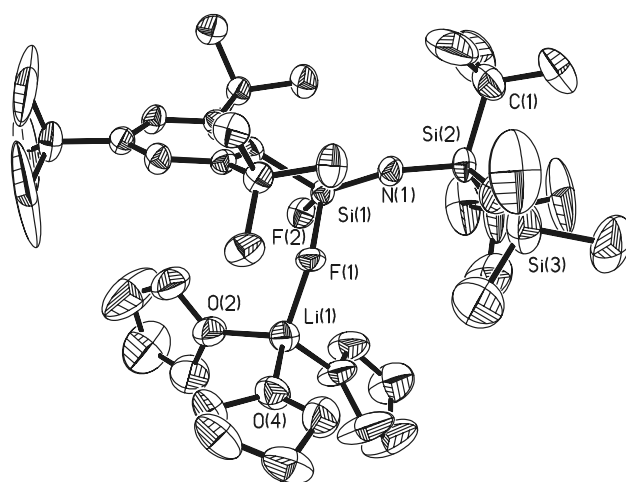
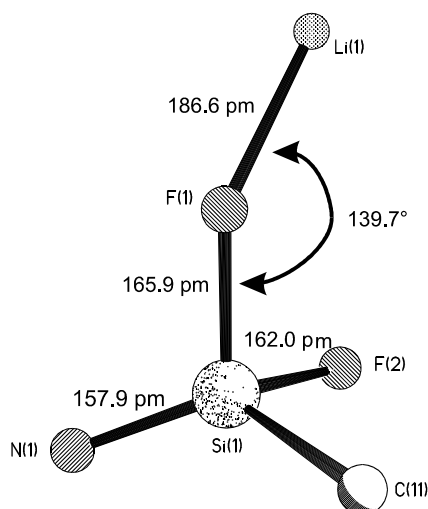
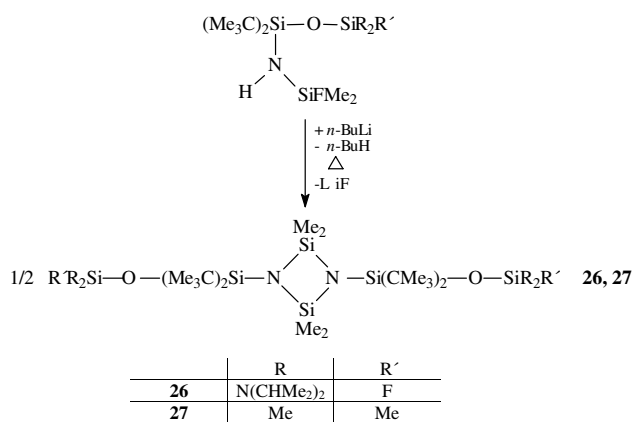


Fig. 17. Structure of **25**; selected bond lengths (pm) and angles ($^{\circ}$): Si(1)–N(1) 157.9(4), Si(1)–F(2) 162.0(3), Si(1)–F(1) 165.9(4), F(1)–Li(1) 186.6(1), O(1)–Si(3) 159.6(6), O(1)–Si(2) 165.3(5), N(1)–Si(2) 163.2(4), N(1)–Si(1)–F(1) 113.5(2), F(2)–Si(1)–F(1) 94.9(2), N(1)–Si(1)–C(11) 127.7(2), Si(1)–F(1)–Li(1) 139.7(4), Si(3)–O(1)–Si(2) 172.6(4), N(1)–Si(2)–O(1) 112.9(2), Si(1)–N(1)–Si(2) 167.2(3).

Fig. 18. Part of the structure of **25**.

(12)

Crystal structure of $[(\text{Me}_2\text{HC})_2\text{N}_2\text{SiF}-\text{O}-\text{Si}(\text{CMe}_3)_2-\text{N}-\text{SiMe}_2]_2$ (**26**). The cyclodisilazane (**26**) crystallizes from *n*-hexane in the space group $P\bar{1}$ (see Fig. 19).

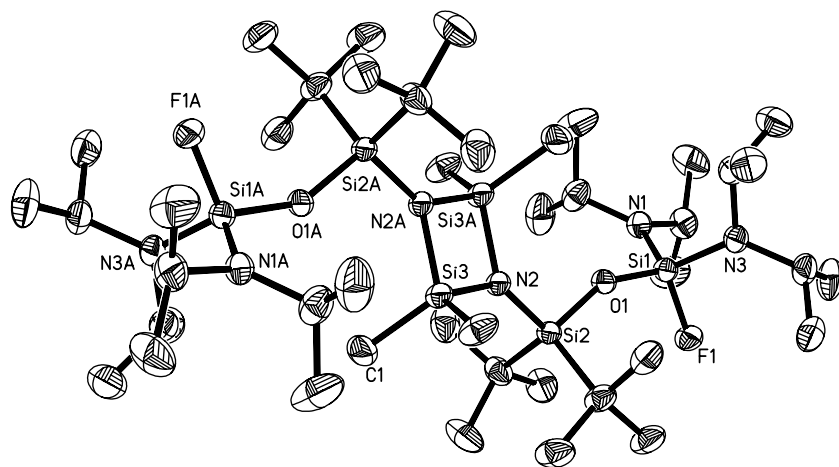
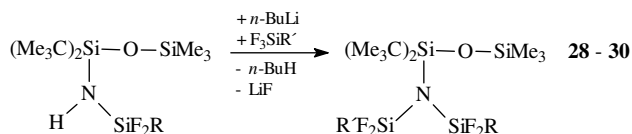


Fig. 19. Structure of **26**; selected bond lengths (pm) and angles ($^\circ$): Si(1)–F(1) 159.4(2), Si(1)–O(1) 162.4(2), Si(1)–N(3) 170.1(2), Si(2)–N(2) 173.4(2), Si(3)–N(2) 175.1(2), Si(3)–Si(3A) 246.6(2); O(1)–Si(2)–N(2) 107.2(9), N(2)–Si(3)–N(2A) 90.5(9), Si(1)–O(1)–Si(2) 150.7(1), Si(2)–N(2)–Si(3) 138.3(1), Si(2)–N(2)–Si(3A) 132.2(1), Si(3)–N(2)–Si(3A) 89.6(9).

The exocyclic Si–N bond lengths are larger than the endocyclic ones. The four-membered (Si–N)₂ ring is planar, the sum of the angles of the all N-atoms is measured with 360 $^\circ$.

2.5.2. Synthesis of 1,1-bis(silylamino)-1,3-disiloxanes

Regarding quantum chemical calculations (Fig. 11) and the experiments, it was expected that lithium salts of 1-silylamino-1,3-disiloxanes react with further fluoro-silanes under retention of the configuration to give 1,1-bis(silylamino)-1,3-disiloxanes.



	28	29	30
R	Ph	CMe ₃	Me
R'	Ph	Me	Me

(13)

Crystal structure of 1,1-Bis(difluoro-phenylsilyl)amino-1,3-disiloxane (**28**). **28** crystallizes from *n*-hexane in the triclinic crystal system, space group $P\bar{1}$. Due to the electron withdrawing effect of the SiF₂ unit, there are two short Si–N bond lengths (170.4, 171.0 pm) and one stretched Si–N bond (179.2 pm), while the nitrogen atom has a planar environment (see Fig. 20).

3. Experimental

All experiments were performed in oven-dried glass ware using standard inert atmosphere and vacuum-line techniques. The NMR spectra were recorded with SiMe₄ and C₆F₆ as internal and MeNO₂ as external references. The compounds were isolated analytically pure.

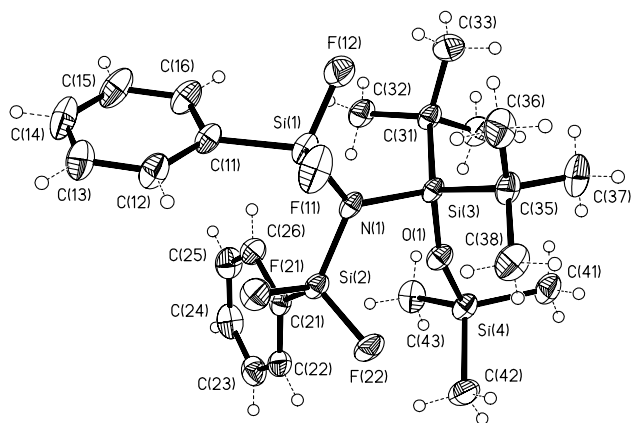


Fig. 20. Structure of **28**; selected bond lengths (pm) and angles ($^{\circ}$): Si(1)–F(11) 157.4(2), Si(1)–N(1) 171.0(2), Si(2)–N(1) 170.4(3), Si(3)–N(1) 179.2(2), Si(3)–O(1) 164.3(2); Si(2)–N(1)–Si(1) 115.6(1), Si(2)–N(1)–Si(3) 117.2(1), Si(1)–N(1)–Si(3) 126.7(1), Si(4)–O(1)–Si(3) 162.1(2), F(11)–Si(1)–F(12) 105.5(1).

3.1. Compounds 1–8

To a solution of 0.1 mol of amino-di-*tert*-butylsilane in 200 ml *n*-hexane the equivalent *n*-butyllithium (23% in *n*-hexane) was added and heated under reflux for 1 h. Then the corresponding halosilane (**1**: 0.1 mol FSiH(CMe₃)₂, room temperature, **2**: 0.1 mol FSiMe₂Ph, room temperature, **3**: 0.1 mol F₃SiPh, -30°C , **4**: 0.1 mol F₃SiC(SiMe₃)₃, room temperature, **5**: 0.1 mol F₃Si-2,2,6,6-tetramethylpiperidine, room temperature, **6**: 0.05 mol SiF₄, -78°C , **7**: 0.033 mol SiF₄, -78°C , **8**: 0.025 mol SiF₄, -78°C) was added. All reaction mixtures were heated for 2 h. After separating the solvent the products were condensed into a cooled trap. Compound **1–8** were purified by distillation; compounds **4** and **8** crystallized from *n*-hexane.

3.1.1. 1-Amino-1,1,3,3-tetra-*tert*-butyl-1,3-disiloxane (**1**)

B.p. $61^{\circ}\text{C}/0.02$ mbar. Yield: 83%. NMR (CDCl₃): ¹H δ 4.51 SiH (1H), 0.95 C(CH₃)₃ (18H), 0.96 C(CH₃)₃ (18H); ¹³C δ 28.26 C(CH₃)₃, 27.60 C(CH₃)₃, 20.48 C(CH₃)₃, 20.18 C(CH₃)₃; ¹⁵N δ -370.81 (t, NH₂, ¹J_{NH} = 73.5 Hz); ²⁹Si δ 5.17 SiH, -12.46 SiN. C₁₆H₃₉NOSi₂, 317.66 g/mol, MS (E.I.) *m/z* 317 (1%) [M]⁺, 260 (100%) [M – CMe₃]⁺.

3.1.2. 1-Amino-1,1-di-*tert*-butyl-3,3-dimethyl-3-phenyl-1,3-disiloxane (**2**)

B.p. $96^{\circ}\text{C}/0.009$ mbar. Yield: 88%. NMR (CDCl₃): ¹H δ 7.72–7.43 C₆H₅ (5H), 1.07 C(CH₃)₃ (18H), 0.79 NH₂ (2H), 0.50 CH₃ (6); ¹³C δ 140.08 C₄, 133.52 C_{2,6}, 133.15 C₁, 127.64 C_{3,5}, 27.83 C(CH₃)₃, 19.71 C(CH₃)₃ 1.01 CH₃; ¹⁵N δ -373.50 (t, NH₂, ¹J_{NH} = 73.1 Hz); ²⁹Si δ -3.87 Si(C₆H₅), -10.98 SiC(CH₃)₃. C₁₆H₃₁NOSi₂, 309.59 g/mol, MS (E.I.) *m/z* 294 (4%) [M – Me]⁺, 252 (100%) [M – CMe₃]⁺.

3.1.3. 1-Amino-1,1-di-*tert*-butyl-3,3-difluoro-3-phenyl-1,3-disiloxane (**3**)

B.p. $60^{\circ}\text{C}/0.03$ mbar. Yield: 78%. NMR (CDCl₃): ¹H δ 7.75–7.35 C₆H₅ (5H), 1.03 C(CH₃)₃ (18H); ¹³C δ 134.39 C_{2,6} (t, ³J_{CF} = 1.2 Hz), 131.82 C₄, 128.22 C_{3,5} (t, ⁴J_{CF} = 0.8 Hz), 126.11 C₁ (t, ²J_{CF} = 29.7 Hz), 27.43 C(CH₃)₃, 19.53 C(CH₃)₃; ¹⁹F δ 25.67; ¹⁵N δ -373.50 NH₂ (t, ¹J_{NH} = 74.9 Hz); ²⁹Si δ -7.33 SiNH₂, -74.76 SiF₂ (t, ¹J_{SiF} = 255.5 Hz). C₁₄H₂₅F₂NOSi₂, 317.52 g/mol, MS (E.I.) *m/z* 260 (68%) [M – CMe₃]⁺.

3.1.4. 1-Amino-1,1-di-*tert*-butyl-3,3-difluoro-3-(tris(trimethylsilyl)methyl)-1,3-disiloxane (**4**)

B.p. $130^{\circ}\text{C}/0.02$ mbar. Yield: 87%. NMR (CDCl₃): ¹H δ 1.04 C(CH₃)₃ (18H), 0.92 NH (2H) 0.27 CH₃ (3H); ¹³C δ 27.89 C(CH₃)₃ (t, ⁵J_{CF} = 0.8 Hz), 19.84 C(CH₃)₃, 4.14 CH₃ (t, ⁴J_{CF} = 1.0 Hz); ¹⁹F δ 48.26, ¹⁵N δ -372.41 NH₂, ²⁹Si δ -0.81 Si(CH₃)₃ (t, ³J_{SiF} = 2.7 Hz), -6.37 SiNH₂, -61.16 SiF₂ (t, ¹J_{SiF} = 271.1 Hz). C₁₈H₄₇F₂NOSi₅, 472.00 g/mol, MS (E.I.) *m/z* 456 (38%) [M – Me]⁺, 414 (100%) [M – CMe₃]⁺.

3.1.5. 1-Amino-1,1-di-*tert*-butyl-3,3-difluoro-3-(2,2,6,6-tetramethylpiperidine)-1,3-disiloxane (**5**)

B.p. $86^{\circ}\text{C}/0.006$ mbar. Yield: 70%. NMR (CDCl₃): ¹H δ 1.65–1.49 C_{3,4,5}H₂ (6H), 1.30 CH₃ (t, ⁴J_{HF} = 1.21 Hz, 12H), 1.00 C(CH₃)₃ (18H); ¹³C δ 51.95 C_{2,6} (t, ³J_{CF} = 0.98 Hz), 41.46 C_{3,5} (t, ⁴J_{CF} = 2.37 Hz), 31.61 CH₃ (t, ⁴J_{CF} = 2.49 Hz), 27.49 C(CH₃)₃, 19.57 C(CH₃)₃, 17.22 C₄; ¹⁹F δ 35.66; ¹⁵N δ -373.96 NH₂ (t, ¹J_{NH} = 73.35 Hz); ²⁹Si δ -8.35 SiC(CH₃)₃, -83.86 SiF₂ (t, ¹J_{SiF} = 215.89 Hz). C₁₇H₃₈F₂N₂OSi₂, 380.66 g/mol, MS (E.I.) *m/z* 380 (2%) [M]⁺, 356 (100%) [M – Me]⁺, 323 (54%) [M – CMe₃]⁺.

3.1.6. 1,5-Diamino-1,1,5,5-tetra-*tert*-butyl-3,3-difluoro-1,3,5-trisiloxane (**6**)

B.p. $74^{\circ}\text{C}/0.008$ mbar. Yield: 12%. NMR (CDCl₃): ¹H δ 1.00 C(CH₃)₃ (36H); ¹³C δ 27.45 C(CH₃)₃, 19.58 C(CH₃)₃; ¹⁹F δ 13.07; ²⁹Si δ -8.16 SiC(CH₃)₃, -108.42 SiF₂ (t, ¹J_{SiF} = 170.1 Hz). C₁₆H₄₀F₂N₂O₂Si₃, 414.75 g/mol, MS (E.I.) *m/z* 357 (18%) [M – CMe₃]⁺.

3.1.7. Fluoro-tris(amino-di-*tert*-butyl)siloxisilane (**7**)

B.p. $127^{\circ}\text{C}/0.006$ mbar. Yield: 8%. NMR (CDCl₃): ¹H δ 0.99 C(CH₃)₃ (54H); ¹³C δ 27.66 C(CH₃)₃ (d, ⁵J_{CF} = 0.5 Hz), 19.67 C(CH₃)₃ (d, ⁴J_{CF} = 0.3 Hz); ¹⁹F δ 26.01; ¹⁵N δ -372.97 NH₂ (t, ¹J_{NH} = 73.4 Hz); ²⁹Si δ -9.60 SiC(CH₃)₃ (d, ³J_{SiF} = 0.3 Hz), -107.88 SiF (d, ¹J_{SiF} = 173.9 Hz). C₂₄H₆₀FN₃O₃Si₄, 570.09 g/mol, MS (E.I.) *m/z* 569 (1%) [M]⁺, 512 (100%) [M – CMe₃]⁺.

3.1.8. 4,4,6,6-Tetra-*tert*-butyl-1,3-dioxo-5-aza-2,4,6-trisilacyclohexane-(2')-spiro-(2')-4', 4', 6', 6'-tetra-*tert*-butyl-1', 3'-dioxo-5'-aza-2', 4', 6'-trisilacyclohexane (**8**)

Melting point (m.p.) >240 °C. Yield: 26%. $C_{32}H_{74}N_2O_4Si_5$, 691.37 g/mol, MS (E.I.) m/z [u] 633 (100%) $[M - CMe_3]^+$.

3.2. Compounds **10**, **18–21**

0.05 mol $(Me_3C)_2Si(NH_2)OSiMe_3$ in 150 ml *n*-hexane were treated with 0.05 mol *n*-butyllithium (23% in *n*-hexane) and heated under reflux for 1 h. Then the halosilane (**10**: 0.05 mol $FSiMe_2Ph$, room temperature, **18**: 0.05 mol F_3SiCMe_3 , –30 °C, **19**: 0.05 mol F_3SiPh , –30 °C, **20**: 0.05 mol $F_3SiN(SiMe_3)_2$, room temperature, **21**: 0.05 mol $F_3Si-2,4,6-(CMe_2)_3C_6H_2$) was added at the mentioned temperature. The mixture was heated under reflux for 2 h (**21**: with 50 ml thf, 8 h under reflux). After separating the solvent the products were condensed into a cooled trap. Compound **10**, **18–21** were purified by distillation; Single crystals of **20** and **21** were obtained by recrystallization from *n*-hexane.

3.2.1. 1-(Trimethylsilyl)amino-1,1-di-*tert*-butyl-3,3-dimethyl-3-phenyl-1,3-disiloxane (**10**)

B.p. 82 °C/0.005 mbar. Yield: 88%. NMR ($CDCl_3$): 1H δ 7.8–7.5 C_6H_5 (5H), 1.14 $C(CH_3)_3$ (18H), 0.54 $OSi(CH_3)_2$ (6H), 0.34 $NSi(CH_3)_3$ (9H); 141.91 C_4 , 133.31 $C_{2,6}$, 128.93 C_1 , 127.76 $C_{3,5}$, 28.13 $C(CH_3)_3$, 20.93 $C(CH_3)_3$, 2.65 $NSiCH_3$, 1.73 $OSiCH_3$; ^{15}N δ –363.14 NH (d, $^1J_{NH} = 64.5$ Hz); ^{29}Si δ 5.56 $Si(CH_3)_3$, –4.48 $Si(CH_3)_2(C_6H_5)$, –9.49 $Si(CH_3)_3$. $C_{19}H_{39}NOSi_3$, 381.78 g/mol, MS (E.I.) m/z 366 (15%) $[M - Me]^+$, 324 (100%) $[M - CMe_3]^+$.

3.2.2. 1-(*tert*-Butyldifluorosilyl)amino-1,1-di-*tert*-butyl-3,3,3-trimethyl-1,3-disiloxane (**18**)

B.p. 64 °C/0.02 mbar. Yield: 64%. NMR ($CDCl_3$): 1H δ 1.05 $FSiC(CH_3)_3$ (t, $^4J_{HF} = 0.94$ Hz, 9H), 1.00 $OSi(CH_3)_3$ (18H), 0.15 $Si(CH_3)_3$ (9H); ^{13}C δ 27.55 $OSi(CH_3)_3$, 25.68 $FSiC(CH_3)_3$, 20.63 $OSi(CH_3)_3$, 16.74 $FSiC(CH_3)_3$ (t, $^2J_{CF} = 19.8$ Hz), 1.90 $SiCH_3$ (t, $^6J_{CF} = 0.7$ Hz); ^{19}F δ 20.11 F (d, $^3J_{FH} = 4.5$ Hz); ^{15}N δ –365.13 NH (t, $^2J_{NF} = 5.5$ Hz); ^{29}Si δ 7.00 $Si(CH_3)_3$, –10.68 $Si(C(CH_3)_3)_2$ (t, $^3J_{SiF} = 1.0$ Hz), –34.87 SiF_2 (t, $^1J_{SiF} = 284.3$ Hz). $C_{15}H_{37}F_2NOSi_3$, 369.71 g/mol, MS (E.I.) m/z 369 (1%) $[M]^+$, 354 (18%) $[M - Me]^+$, 312 (100%) $[M - CMe_3]^+$.

3.2.3. 1-(Difluorophenylsilyl)amino-1,1-di-*tert*-butyl-3,3,3-trimethyl-1,3-disiloxane (**19**)

B.p. 84 °C/0.007 mbar. Yield: 86%. NMR ($CDCl_3$): 1H δ 7.82–7.43 C_6H_5 (5H), 1.14 $C(CH_3)_3$ (18H), 0.26 CH_3 (9H); 134.44 $C_{2,6}$ (t, $^3J_{CF} = 1.2$ Hz), 131.66 C_4 (t, $^5J_{CF} = 0.5$ Hz), 129.01 C_1 (t, $^2J_{CF} = 26.6$ Hz), 128.26 $C_{3,5}$ (t, $^4J_{CF} = 0.6$ Hz), 27.14 $C(CH_3)_3$, 20.68 $C(CH_3)_3$

(t, $^4J_{CF} = 0.5$ Hz), 1.94 CH_3 (t, $^6J_{CF} = 0.7$ Hz); ^{19}F δ 28.57 F (d, $^3J_{FH} = 4.9$ Hz); ^{15}N δ –358.41 NH (t, $^3J_{NF} = 3.9$ Hz); ^{29}Si δ 7.49 $Si(CH_3)_3$, –10.16 $SiC(CH_3)_3$ (t, $^3J_{SiF} = 0.8$ Hz), –46.92 $SiF_2(C_6H_5)$ (t, $^1J_{SiF} = 259.8$ Hz). $C_{17}H_{33}F_2NOSi_3$, 389.70 g/mol, MS (E.I.) m/z [u] 374 (8%) $[M - Me]^+$, 332 (35%) $[M - CMe_3]^+$.

3.2.4. 1-Bis(trimethylsilyl)amino-difluorosilylamino-1,1-di-*tert*-butyl-3,3,3-trimethyl-1,3-disiloxane (**20**)

M.p. 56 °C. Yield: 83%. NMR ($CDCl_3$): 1H δ 0.98 $SiC(CH_3)_3$ (18H), 0.22 $NSi(CH_3)_3$ (18H), 0.17 $OSi(CH_3)_3$ (9H); ^{13}C δ 27.60 $SiC(CH_3)_3$, 20.58 $SiC(CH_3)_3$ (t, $^4J_{CF} = 0.9$ Hz), 3.75 $NSi(CH_3)_3$ (t, $^4J_{CF} = 1.4$ Hz), 1.94 $OSi(CH_3)_3$ (t, $^6J_{CF} = 1.2$ Hz); ^{19}F δ 39.27 (d, $^3J_{FH} = 3.3$ Hz); ^{15}N δ –355.30 NH (t, $^2J_{NF} = 8.5$ Hz); ^{29}Si δ 6.88 $OSi(CH_3)_3$, 5.55 $NSi(CH_3)_2$ (t, $^3J_{SiF} = 1.3$ Hz), –11.30 $SiC(CH_3)_3$ (t, $^3J_{SiF} = 1.1$ Hz), –61.04 SiF_2 (t, $^1J_{SiF} = 221.6$ Hz). $C_{17}H_{46}F_2N_2OSi_5$, 472.98 g/mol, MS (E.I.) m/z [u] 457 (30%) $[M - Me]^+$, 415 (100%) $[M - CMe_3]^+$.

3.2.5. 1-Difluoro(2,4,6-tri-*tert*-butylphenyl)silylamino-1,1-di-*tert*-butyl-3,3,3-trimethyl-1,3-disiloxane (**21**)

B.p. 148 °C/0.01 mbar, m.p. 87 °C. Yield: 78%. NMR ($CDCl_3$): 1H δ 7.39 $C_{3,5}H$ (2H), 1.50 $C_{2,6}C(CH_3)_3$ (18H), 1.30 $C_4C(CH_3)_3$ (9H), 1.03 $SiC(CH_3)_3$ (18H), 0.17 $Si(CH_3)_3$ (9H); ^{13}C δ 160.47 $C_{2,6}$ (t, $^3J_{CF} = 1.3$ Hz), 151.48 C_4 , 122.91 $C_{3,5}$, 120.19 C_1 (t, $^2J_{CF} = 20.0$ Hz), 39.02 $C_{2,6}C(CH_3)_3$ (t, $^4J_{CF} = 0.6$ Hz), 34.67 $C_4C(CH_3)_3$, 33.57 $C_{2,6}C(CH_3)_3$ (t, $^5J_{CF} = 2.4$ Hz), 31.07 $C_4C(CH_3)_3$, 27.79 $SiC(CH_3)_3$, 20.77 $SiC(CH_3)_3$, 2.06 $SiCH_3$; ^{19}F δ 47.52 F (d, $^3J_{FH} = 6.3$ Hz); ^{15}N δ –346.03 NH (t, $^2J_{NF} = 6.4$ Hz); ^{29}Si δ 6.49 $Si(CH_3)_3$, –11.83 $SiC(CH_3)_3$ (t, $^3J_{SiF} = 1.0$ Hz), –46.52 SiF_2 (t, $^1J_{SiF} = 249.1$ Hz). $C_{29}H_{57}F_2NOSi_3$, 558.02 g/mol, MS (E.I.) m/z 557 (1%) $[M]^+$, 542 (15%) $[M - Me]^+$, 500 (75%) $[M - CMe_3]^+$.

3.3. Compounds **9**, **11–17**

0.05 mol of compound **2** (**9**), $(Me_3C)_2Si(NH_2)O-SiF_2CMe_3$ (**11–15**), $(Me_3C)_2Si(NH_2)OSiF(N(CHMe_2)_2)_2$ (**16**) or compound **1** (**17**) are solved in 150 ml *n*-hexane and treated with the equivalent *n*-butyllithium (23% in *n*-hexane). After 1 h heating under reflux the corresponding halosilane (**9**: 0.05 mol $ClSiMe_3$, room temperature, **11**: 0.05 mol F_3SiMe , –50 °C, **12**, **13**: 0.05 mol F_2SiMe_2 , –20 °C, **14**, **15**: 0.05 mol F_3SiPh , –20 °C, **16**: 0.05 mol F_2SiMe_2 , –20 °C, **17**: 0.05 mol $F_2Si(CMe_3)_2$, room temperature) was added. To the reaction mixtures of **9** and **17** were given 50 ml thf and they were heated under reflux for 3 h. The reaction mixtures of **11–16** were warmed to room temperature and heated under reflux for 1 h. All products were condensed into a cooled trap and purified by distillation. Compound **17** was crystallized from *n*-hexane.

3.3.1. 1-(Dimethylphenylsilyl)amino-1,1-di-tert-butyl-3,3,3-trimethyl-1,3-disiloxane (9)

B.p. 92 °C/0.006 mbar. Yield: 24%. NMR (CDCl₃): ¹H δ 7.73–7.41 C₆H₅ (5H), 1.01 C(CH₃)₃ (18H), 0.55 Si(CH₃)₂C₆H₅ (6H), 0.50 Si(CH₃)₃ (9H); ¹³C δ 139.48 C₄, 133.69 C_{2,6}, 129.45 C₁, 127.72 C_{3,5}, 28.19 C(CH₃)₃, 20.19 C(CH₃)₃, 2.94 Si(CH₃)₃, 1.23 Si(CH₃)₂C₆H₅; ¹⁵N δ –360.77 NH (d, ¹J_{NH} = 63.9 Hz); ²⁹Si δ 2.17 Si(CH₃)₃, –4.09 Si(CH₃)₂C₆H₅, –9.12 SiC(CH₃)₃. C₁₉H₃₉NOSi₃, 381.78 g/mol, MS (E.I.) *m/z* 366 (8%) [M – Me]⁺, 324 (100%) [M – CMe₃]⁺.

3.3.2. 1-(tert-Butyldifluorosilyl)amino-1,1-di-tert-butyl-3,3-difluoro-3-methyl-1,3-disiloxane (11)

B.p. 62 °C/0.5 mbar. Yield: 64%. NMR (CDCl₃): ¹H δ 1.04 FSiC(CH₃)₃ (t, ⁴J_{HF} = 0.88 Hz, 9H), 1.01 OSiC(CH₃)₃ (18H), 0.36 CH₃ (t, ³J_{HF} = 4.16 Hz, 3H); ¹³C δ 27.16 OSiC(CH₃)₃, 25.49 FSiC(CH₃)₃, 20.61 OSiC(CH₃)₃, 16.79 FSiC(CH₃)₃ (t, ²J_{CF} = 19.6 Hz), –8.01 CH₃ (t/t, ²J_{CF} = 25.3 Hz, ⁶J_{CF} = 1.3 Hz); ¹⁹F δ 32.10 FSiCH₃ (q/t, ³J_{FH} = 4.2 Hz, ⁶J_{FF} = 1.5 Hz), 19.03 FSiC(CH₃)₃ (d/t, ³J_{FH} = 5.7 Hz, ⁶J_{FF} = 1.5 Hz); ²⁹Si δ –6.02 OSiC(CH₃)₃, –34.76 SiCH₃ (t, ¹J_{SiF} = 286.6 Hz), –59.90 FSiC(CH₃)₃ (t, ¹J_{SiF} = 259.7 Hz). C₁₃H₃₁F₄NOSi₃, 377.64 g/mol, MS (E.I.) *m/z* 377 (1%) [M]⁺, 320 (30%) [M – CMe₃]⁺.

3.3.3. 2-(tert-Butyldifluorosilyl)amino-1,1-di-tert-butyl-3-fluoro-3,3-dimethyl-1,3-disiloxane (12)

B.p. 42 °C/0.04 mbar. Yield: 47%. NMR (CDCl₃): ¹H δ 1.04 FSiC(CH₃)₃ (t, ⁴J_{HF} = 0.86 Hz, 9H), 1.01 OSiC(CH₃)₃ (18H), 0.25 CH₃ (d, ³J_{HF} = 6.53 Hz, 6H); ¹³C δ 27.40 OSiC(CH₃)₃, 25.62 FSiC(CH₃)₃, 20.68 OSiC(CH₃)₃, 16.80 FSiC(CH₃)₃ (t, ²J_{CF} = 19.7 Hz), 0.23 CH₃ (d, ²J_{CF} = 19.5 Hz); ¹⁹F δ 32.61 FSiO (sept/t, ³J_{FH} = 6.5 Hz, ⁶J_{FF} = 1.1 Hz), 19.10 FSiN (d/d, ³J_{FH} = 5.8 Hz, ⁶J_{FF} = 1.1 Hz); ²⁹Si δ –8.34 Si(C(CH₃)₃)₂ (d/t, ³J_{SiF} = 1.0 Hz, ³J_{SiF} = 0.9 Hz), –9.16 SiF(CH₃)₂ (d, ¹J_{SiF} = 277.2 Hz), –34.80 SiF₂C(CH₃)₃ (t, ¹J_{SiF} = 289.3 Hz). C₁₄H₃₄F₃NOSi₃, 373.68 g/mol, MS (E.I.) *m/z* 316 (55%) [M – CMe₃]⁺.

3.3.4. 1-(Fluorodimethylsilyl)amino-1,1,3-tri-tert-butyl-3,3-difluoro-1,3-disiloxane (13)

B.p. 42 °C/0.04 mbar. Yield: 21%. NMR (CDCl₃): ¹H δ 1.09 FSiC(CH₃)₃ (t, ⁴J_{HF} = 0.98 Hz, 9H), 1.03 NSiC(CH₃)₃ (18H), 0.23 CH₃ (d, ³J_{HF} = 6.23 Hz, 6H); ¹³C δ 27.53 NSiC(CH₃)₃, 25.45 FSiC(CH₃)₃, 20.75 NSiC(CH₃)₃, 15.98 FSiC(CH₃)₃ (t, ²J_{CF} = 21.6 Hz), –1.19 CH₃ (d/t, ²J_{CF} = 19.1 Hz, ⁶J_{CF} = 0.9 Hz); ¹⁹F δ 29.87 FSiN, 19.31 FSiO (d, ⁶J_{FF} = 1.4 Hz); ²⁹Si δ 6.23 SiF(CH₃)₂ (d, ¹J_{SiF} = 276.0 Hz), –8.34 Si(C(CH₃)₃)₂ (t/d, ³J_{SiF} = 1.0 Hz, ³J_{SiF} = 0.9 Hz), –63.49 SiF₂C(CH₃)₃ (t, ¹J_{SiF} = 290.5 Hz). C₁₄H₃₄F₃NOSi₃, 373.68 g/mol, MS (E.I.) *m/z* 316 (55%) [M – CMe₃]⁺.

3.3.5. 1-(tert-Butyldifluorosilyl)amino-1,1-di-tert-butyl-3,3-difluoro-3-phenyl-1,3-disiloxane (14)

B.p. 93 °C/0.008 mbar. Yield: 42%. NMR (CDCl₃): ¹H δ 7.83–7.43 C₆H₅ (5H), 1.12 OSiC(CH₃)₃ (18H), 1.10 SiF₂C(CH₃)₃ (t, ⁴J_{HF} = 0.90 Hz, 9H); ¹³C δ 134.41 C_{2,6}, 131.95 C₄, 128.41 C_{3,5}, 128.25 C₁ (t, ²J_{CF} = 26.2 Hz), 27.28 OSiC(CH₃)₃, 25.42 SiF₂C(CH₃)₃, 20.72 OSiC(CH₃)₃, 16.80 SiF₂C(CH₃)₃ (t, ²J_{CF} = 19.58 Hz); ¹⁹F δ 26.88 FSiC(CH₃)₃ (t, ⁶J_{FF} = 1.8 Hz), 21.16 FSiC(CH₃)₃ (d/t, ³J_{FH} = 5.7 Hz, ⁶J_{FF} = 1.8 Hz); ²⁹Si δ –4.90 OSiC(CH₃)₃, –34.93 SiF₂C(CH₃)₃ (t, ¹J_{SiF} = 287.5 Hz), –75.62 SiF₂(C₆H₅) (¹J_{SiF} = 256.6 Hz). C₁₈H₃₃F₄NOSi₃, 439.71 g/mol, MS (E.I.) *m/z* 382 (82%) [M – CMe₃]⁺, 362 (12%) [M – Ph]⁺.

3.3.6. 1-(Difluorophenylsilyl)amino-1,1,3-tri-tert-butyl-3,3-difluoro-1,3-disiloxane (15)

B.p. 93 °C/0.008 mbar. Yield: 47%. NMR (CDCl₃): ¹H δ 7.83–7.43 C₆H₅ (5H), 1.18 SiF₂C(CH₃)₃ (t, ⁴J_{HF} = 1.01 Hz, 9H), 1.17 NSiC(CH₃)₃ (18H); ¹³C δ 134.50 C_{2,6} (t, ³J_{CF} = 1.3 Hz), 131.94 C₄, 128.28 C_{3,5} (t, ⁴J_{CF} = 0.8 Hz), 125.50 C₁ (t, ²J_{CF} = 29.2 Hz), 27.34 NSiC(CH₃)₃, 25.42 SiF₂C(CH₃)₃, 20.72 NSiC(CH₃)₃, 15.92 SiF₂C(CH₃)₃ (t, ²J_{CF} = 19.6 Hz); ¹⁹F δ 30.38 FSi(C₆H₅) (d/t, ³J_{FH} = 5.4 Hz, ⁶J_{FF} = 1.9 Hz), 20.03 FSiC(CH₃)₃ (t, ⁶J_{FF} = 1.9 Hz); ²⁹Si δ –5.12 NSiC(CH₃)₃, –47.27 SiF₂(C₆H₅) (t, ¹J_{SiF} = 287.5 Hz), –63.04 SiF₂C(CH₃)₃ (t, ¹J_{SiF} = 256.6 Hz). C₁₈H₃₃F₄NOSi₃, 439.71 g/mol, MS (E.I.) *m/z* 382 (82%) [M – CMe₃]⁺, 362 (12%) [M – Ph]⁺.

3.3.7. 1-(Fluorodimethylsilyl)amino-3,3-bis-(di-isopropyl)amino-1,1-di-tert-butyl-3-fluoro-1,3-disiloxane (16)

B.p. 112 °C/0.02 mbar. Yield: 68%. NMR (CDCl₃): ¹H δ 3.41 CH(CH₃)₂ (sept, ³J_{HH} = 6.73 Hz, 4H), 1.22 CH(CH₃)₂ (d, ³J_{HH} = 6.84 Hz, 12H), 1.20 CH(CH₃)₂ (d, ³J_{HH} = 6.80 Hz, 12H), 1.06 C(CH₃)₃ (6H), 0.24 CH₃ (d, ³J_{HF} = 6.11 Hz, 6H); ¹³C δ 44.83 CH(CH₃)₂, 27.93 C(CH₃)₃ (t, ⁵J_{CF} = 0.9 Hz), 24.71 CH(CH₃)₂ (d, ⁴J_{CF} = 1.4 Hz), 24.28 CH(CH₃)₂ (d, ⁴J_{CF} = 1.2 Hz), 20.84 C(CH₃)₃, 0.91 CH₃ (d, ²J_{CF} = 19.7 Hz); ¹⁹F δ 37.76 FSiO, FSiN 30.85; ¹⁵N δ –345.85 NH (d/d, ¹J_{NH} = 62.0 Hz, ²J_{NF} = 6.5 Hz); ²⁹Si δ 3.79 Si(CH₃)₂ (d, ¹J_{SiF} = 274.7 Hz), –7.75 SiC(CH₃)₃, –67.93 SiNCH(CH₃)₂ (d, ¹J_{SiF} = 230.8 Hz). C₂₂H₅₃F₂N₃O₂Si₃, 497.93 g/mol, MS (E.I.) *m/z* 497 (4%) [M]⁺, 482 (25%) [M – Me]⁺, 440 (28%) [M – CMe₃]⁺.

3.3.8. 1-(Di-tert-butylfluorosilyl)amino-1,1,3,3-tetra-tert-butyl-1,3-disiloxane (17)

B.p. 122 °C/0.01 mbar, m.p. 93 °C. Yield: 48%. NMR (CDCl₃): ¹H δ 4.29 SiH (1H), 1.09 HSiC(CH₃)₃ (18H), 1.06 FSiC(CH₃)₃ (d, ⁴J_{HF} = 0.93 Hz, 18H), 1.05 Si(C(CH₃)₃)₂ (18H); ¹³C δ 28.58 FSiC(CH₃)₃ (d, ³J_{CF} = 2.6 Hz), 28.10 HSiC(CH₃)₃, 27.78 Si(C(CH₃)₃)₂

(d, $^5J_{CF} = 0.6$ Hz), 21.43 HSiC(CH₃)₃, 21.08 FSiC(CH₃)₃ (d, $^2J_{CF} = 15.1$ Hz), 20.46 Si(C(CH₃)₃)₂; ^{19}F δ 0.90 F (d, $^3J_{FH} = 13.7$ Hz); ^{15}N δ -362.00 NH (d, $^2J_{NF} = 6.2$ Hz); ^{29}Si δ 4.15 SiH, 2.61 SiF (d, $^1J_{SiF} = 300.7$ Hz), -12.05 Si(C(CH₃)₃)₂ (d, $^3J_{SiF} = 1.1$ Hz). C₂₄H₅₆FNOSi₃, 477.96 g/mol, MS (E.I.) *m/z* 420 (100%) [M - CMe₃]⁺.

3.4. Compound 22

To a solution of 0.05 mol (Me₃C)₂Si(NH₂)OSiF₂Me in 150 ml *n*-hexane are 0.05 mol *n*-butyllithium (23% in *n*-hexane) added. After heating under reflux for 1 h and separating the solvent, the reaction mixture was heated to reflux for another 2 h. Compound **22** was condensed into a cooled trap and then crystallized from *n*-hexane.

3.4.1. 2,2,6,6-Tetra-*tert*-butyl-4,8-difluoro-4,8-dimethyl-1,5-dioxo-3,7-diaza-2,4,6,8-tetrasilacyclooctane (22)

B.p. 105 °C/0.01 mbar, m.p. 166 °C. Yield: 48%. NMR (CDCl₃): 1H δ 1.00 C(CH₃)₃*trans* (18H), 0.99 C(CH₃)₃*trans* (18H), 0.98 C(CH₃)₃*cis* (18H), 0.97 C(CH₃)₃*cis* (18H), 0.24 CH₃*cis* (d, $^3J_{HF} = 4.69$ Hz, 6H), 0.23 CH₃*trans* (d, $^3J_{HF} = 4.69$ Hz, 6H); δ ^{13}C 27.73 C(CH₃)₃*cis*, 27.51 C(CH₃)₃*trans*, 27.29 C(CH₃)₃*cis* (d, $^5J_{CF} = 1.5$ Hz), 20.67 C(CH₃)₃*cis* (d, $^4J_{CF} = 1.6$ Hz), 20.65 C(CH₃)₃*cis*, 20.18 C(CH₃)₃*trans*, -2.41 CH₃*trans* (d, $^2J_{CF} = 31.0$ Hz), -2.48 CH₃*cis* (d, $^2J_{CF} = 30.9$ Hz); ^{19}F δ 46.43 F_{*cis*}, 45.51 F_{*trans*}; ^{29}Si δ -9.28 SiC(CH₃)₃*cis*, -9.33 SiC(CH₃)₃*trans*, -42.36 SiF_{*cis*} (d, $^1J_{SiF} = 259.3$ Hz), -42.58 SiF_{*trans*} (d, $^1J_{SiF} = 258.6$ Hz). C₁₈H₄₄F₂N₂O₂Si₄, 470.89 g/mol, MS (E.I.) *m/z* 470 (2%) [M]⁺, 413 (100%) [M - CMe₃]⁺.

3.5. Compounds 23–25

A solution of 0.01 mol of compound **20** (**23**, **25**), respectively, **21** (**24**) in 100 ml *n*-hexane (**23**, **24**), respectively, thf (**25**) was treated with 0.01 mol *n*-butyllithium (23% in *n*-hexane). The products were purified by crystallisation from *n*-hexane.

3.5.1. Lithium-1-difluoro(bis(trimethylsilyl)amino)-silylamido-1,1-di-*tert*-butyl-3,3,3-trimethyl-1,3-disiloxane (23)

(C₁₇H₄₅F₂LiN₂OSi₅)₂, (478.92)₂ g/mol.

3.5.2. Lithium-1-difluoro(2,4,6-tri-*tert*-butylphenyl)-silylamido-1,1-di-*tert*-butyl-3,3,3-trimethyl-1,3-disiloxane (24)

NMR (C₆D₆): 7Li δ 0.31 (t, $^1J_{LiF} = 32.2$ Hz); ^{19}F δ 57.12 (q, $^1J_{FLi} = 32.1$ Hz). (C₂₉H₅₆F₂LiNOSi₃)₂, (563.96)₂ g/mol.

3.5.3. Lithium-1-difluoro(2,4,6-tri-*tert*-butylphenyl)-silylamido-1,1-di-*tert*-butyl-3,3,3-trimethyl-1,3-disiloxane (25)

NMR (C₆D₆): 7Li δ -1.16; ^{19}F δ 55.18; ^{29}Si δ -3.11 Si(CH₃)₃, -31.86 SiC(CH₃)₃, -69.53 SiF₂ (t, $^1J_{SiF} = 249.9$ Hz). C₂₉H₅₆F₂LiNOSi₃, 563.96 g/mol.

3.6. Compounds 26 and 27

A solution 0.05 mol of compound **16** (**26**), respectively, (Me₃C)₂Si(NH₂)OSiFMe₂ (**27**) in 150 ml *n*-hexane were treated with 0.05 mol *n*-butyllithium (23% in *n*-hexane) and heated under reflux for 1 h. After evaporating the solvent the mixture was heated to reflux for another 3 h. Compounds **26** and **27** were condensed into a cooled trap before distillation in vacuo. Single crystals of **26** were obtained by recrystallization from *n*-hexane.

3.6.1. 1,3-Bis(1,1-di-*tert*-butyl-3-fluoro-3,3-bis(di-isopropyl)amino)-1,3-disiloxane-2,2,4,4-tetramethyl-2,4-cyclodisilazane (26)

M.p. >250 °C. Yield: 73%. NMR (CDCl₃): 1H δ 3.57 CH(CH₃)₂ (sept, $^3J_{HH} = 6.37$ Hz, 8H), 1.24 CH(CH₃)₂ (d, $^3J_{HH} = 6.47$ Hz, 24H), 1.17 CH(CH₃)₂ (d, $^3J_{HH} = 6.53$ Hz, 24H), 1.05 C(CH₃)₃ (36H), 0.53 CH₃ (12H); ^{13}C δ 45.53 CH(CH₃)₂, 29.19 C(CH₃)₃ (d, $^5J_{CF} = 1.2$ Hz), 25.39 CH(CH₃)₂ (d, $^4J_{CF} = 1.1$ Hz), 25.05 CH(CH₃)₂ (d, $^4J_{CF} = 0.6$ Hz), 21.46 C(CH₃)₃, 8.77 CH₃; ^{19}F δ 34.59; ^{29}Si δ 5.00 Si(CH₃), -11.17 SiC(CH₃)₃, -70.42 SiNCH(CH₃)₂ (d, $^1J_{SiF} = 228.2$ Hz). C₄₄H₁₀₄F₂N₆O₂Si₆, 955.85 g/mol, (E.I.) *m/z* 954 (1%) [M]⁺, 939 (5%) [M - Me]⁺, 897 (100%) [M - CMe₃]⁺.

3.6.2. 1,3-Bis(1,1-di-*tert*-butyl-3,3,3-trimethyl)-1,3-disiloxane-2,2,4,4-tetramethyl-2,4-cyclodisilazane (27)

B.p. 95 °C/0.008 mbar, m.p. 78 °C. Yield: 21%. NMR (CDCl₃): 1H δ 0.96 C(CH₃)₃ (36H), 0.43 NSi(CH₃)₂ (12H), 0.17 OSi(CH₃)₃ (18H); ^{13}C δ 28.45 C(CH₃)₃, 20.84 C(CH₃)₃, 7.85 NSi(CH₃)₂, 3.20 OSi(CH₃)₃; ^{29}Si δ 4.28 OSi(CH₃)₃, 3.66 NSi(CH₃)₂, -12.96 SiC(CH₃)₃. C₂₆H₆₆N₂O₂Si₆, 607.33 g/mol, MS, (E.I.) *m/z* 606 (2%) [M]⁺, 593 (8%) [M - Me]⁺, 549 (100%) [M - CMe₃]⁺.

3.7. Compounds 28–30

0.05 mol of compound **19** (**28**), **18** (**29**), respectively, (Me₃C)₂Si(NH₂)OSiF₂Me (**30**) were solved in 150 ml *n*-hexane and treated with 0.05 mol *n*-butyllithium (23% in *n*-hexane) at -50 °C. After warming the reaction mixtures at room temperature the corresponding halosilane (**28**: 0.05 mol F₃SiPh, 0 °C, **29**, **30**: 0.05 mol F₃SiMe, -50 °C) was added. The solutions were afterwards warmed to room temperature and heated under reflux for 1 h before the products were condensed into

Table 2

Compound	21	22	23	24
Identification code				
Empirical formula	C ₂₉ H ₅₇ F ₂ NOSi ₃	C ₁₈ H ₄₄ F ₂ N ₂ O ₂ Si ₄	C ₃₄ H ₉₀ F ₄ Li ₂ N ₄ O ₂ Si ₁₀	C ₅₈ H ₁₁₂ F ₄ Li ₂ N ₂ O ₂ Si ₆
Formula weight	558.03	470.91	957.88	1127.92
<i>T</i> (K)	203(2)	150(2)	203(2)	200(2)
λ (pm)	71.073	71.073	71.073	71.073
Crystal system	Monoclinic	Triclinic	Monoclinic	Triclinic
Space group	<i>P</i> 2(1)/ <i>n</i>	<i>P</i> $\bar{1}$	<i>P</i> 2(1)/ <i>c</i>	<i>P</i> $\bar{1}$
Unit cell dimensions				
<i>a</i> (pm)	901.15(13)	839.02(17)	934.66(15)	980.6(3)
<i>b</i> (pm)	1319.8(2)	919.31(18)	2617.1(11)	1346.7(9)
<i>c</i> (pm)	2914.3(18)	985.9(2)	1204.1(3)	1404.0(6)
α (°)	90	89.68(3)	90	85.74(6)
β (°)	96.22(2)	72.17(3)	105.059(14)	81.57(2)
γ (°)	90	75.07(3)	90	70.12(2)
<i>V</i> (nm ³)	3.45(1)	0.6768(2)	2.8442(14) nm ³	1.7241(15)
<i>Z</i>	4	1	2	1
Density (calculated) (Mg/m ³)	1.076	1.155	1.118	1.086
Absorption coefficient (mm ⁻¹)	0.169	0.248	0.274	0.169
<i>F</i> (000)	1224	256	1040	616
Crystal size (mm ³)	1.00 × 0.80 × 0.80	1.00 × 0.80 × 0.20	0.80 × 0.80 × 0.30	1.10 × 0.50 × 0.10
θ Range for data collection (°)	3.61–25.04	3.71–25.02	3.50–22.54	3.50–22.53
Index ranges	–10 ≤ <i>h</i> ≤ 10, –15 ≤ <i>k</i> ≤ 15, –34 ≤ <i>l</i> ≤ 34	–9 ≤ <i>h</i> ≤ 9, –10 ≤ <i>k</i> ≤ 10, –11 ≤ <i>l</i> ≤ 11	–10 ≤ <i>h</i> ≤ 9, 0 ≤ <i>k</i> ≤ 20, 0 ≤ <i>l</i> ≤ 12	–10 ≤ <i>h</i> ≤ 10, –14 ≤ <i>k</i> ≤ 14, –5 ≤ <i>l</i> ≤ 15
Reflections collected	8666	3718	3258	4529
Independent reflections (<i>R</i> _{int})	6057 (0.0478)	2379 (0.0661)	3258 (0.0000)	4486 (0.2071)
Completeness	to $\theta = 25.04^\circ$, 99.3%	to $\theta = 25.02^\circ$, 99.5%	to $\theta = 22.54^\circ$, 87.5%	to $\theta = 22.53^\circ$, 99.2%
Maximum and minimum transmission	0.8768 and 0.8493	0.9520 and 0.7892	0.9222 and 0.8104	0.9833 and 0.8360
Refinement method	Full-matrix least-squares on <i>F</i> ²	Full-matrix least-squares on <i>F</i> ²	Full-matrix least-squares on <i>F</i> ²	Full-matrix least-squares on <i>F</i> ²
Data/restraints/parameters	6057/490/343	2379/179/134	3258/0/268	4486/0/352
Goodness-of-fit on <i>F</i> ²	1.026	1.063	1.039	0.997
Final <i>R</i> indices [<i>I</i> > 2 σ (<i>I</i>)]	<i>R</i> ₁ = 0.0673, <i>wR</i> ₂ = 0.1823	<i>R</i> ₁ = 0.0929, <i>wR</i> ₂ = 0.2441	<i>R</i> ₁ = 0.0465, <i>wR</i> ₂ = 0.1466	<i>R</i> ₁ = 0.0557, <i>wR</i> ₂ = 0.1421
<i>R</i> indices (all data)	<i>R</i> ₁ = 0.0765, <i>wR</i> ₂ = 0.1933	<i>R</i> ₁ = 0.1075, <i>wR</i> ₂ = 0.2608	<i>R</i> ₁ = 0.0517, <i>wR</i> ₂ = 0.1547	<i>R</i> ₁ = 0.0676, <i>wR</i> ₂ = 0.1551
Largest difference peak and hole (e Å ⁻³)	0.715 and –0.699	0.722 and –0.727	0.340 and –0.324	0.452 and –0.358

a cooled trap. Compounds **28–30** were purified by distillation. **28** gives single crystals from *n*-hexane.

3.7.1. 1-Bis(difluorophenylsilyl)amino-1,1-di-*tert*-butyl-3,3,3-trimethyl-1,3-disiloxane (**28**)

B.p. 123 °C/0.02 mbar, m.p. 42 °C. Yield: 23%. NMR (CDCl₃): ¹H δ 7.75–7.10 C₆H₅ (10H), 1.12 C(CH₃)₃ (18H), 0.13 CH₃ (9H); ¹³C δ 134.68 C_{2,6}, 131.61 C₄, 128.97 C₁, 128.13 C_{3,5}, 28.48 C(CH₃)₃, 22.27 C(CH₃)₃, 2.41 CH₃; ¹⁹F δ 38.13 SiF₂ (t, ⁴J_{FF} = 2.1 Hz), 27.09 (t, ⁴J_{FF} = 2.1 Hz); ²⁹Si δ 9.31 Si(CH₃)₃, –2.56 SiC(CH₃)₃, –47.38 SiF₂ (t/t, ¹J_{SiF} = 272.4 Hz, ³J_{SiF} = 3.9 Hz), –49.77 SiF₂ (t/t, ¹J_{SiF} = 269.3 Hz, ³J_{SiF} = 3.7 Hz). C₂₃H₃₇F₄NOSi₄, 531.88 g/mol, MS (E.I.) *m/z* 516 (18%) [M – Me]⁺, 474 (100%) [M – CMe₃]⁺.

3.7.2. 1-(*tert*-Butyldifluorosilyl)-(difluoromethylsilyl)amino-1,1-di-*tert*-butyl-3,3,3-trimethyl-1,3-disiloxane (**29**)

B.p. 76 °C/0.004 mbar. Yield: 85%. NMR (CDCl₃): ¹H δ 1.07 F₂SiC(CH₃)₃ (9H), 1.03 SiC(CH₃)₃ (18H), 0.49 F₂SiCH₃ (t, ³J_{HF} = 4.97 Hz, 3H), 1.19 Si(CH₃)₃ (9H); ¹³C δ 28.34 SiC(CH₃)₃ (t, ⁵J_{CF} = 1.9 Hz), 28.02

F₂SiC(CH₃)₃ (t/t, ³J_{CF} = 1.8 Hz, ⁵J_{CF} = 0.8 Hz), 22.13 SiC(CH₃)₃, 19.40 F₂SiC(CH₃)₃ (t, ²J_{CF} = 19.6 Hz), 3.18 Si(CH₃)₃ (t, ⁶J_{CF} = 1.0 Hz), –1.61 (t, ²J_{CF} = 22.8 Hz); ¹⁹F δ 44.82 F₂SiCH₃ (t, ⁴J_{FF} = 3.1 Hz), 36.31 F₂SiC(CH₃)₃ (t, ⁴J_{FF} = 3.1 Hz); ²⁹Si δ 9.32 Si(CH₃)₃, –1.94 SiC(CH₃)₃, –32.57 F₂SiCH₃ (t/t, ¹J_{SiF} = 272.7 Hz, ³J_{SiF} = 4.7 Hz), –35.70 F₂SiC(CH₃)₃ (t/t, ¹J_{SiF} = 297.5 Hz, ³J_{SiF} = 1.8 Hz). C₁₆H₃₉F₄NOSi₄, 449.82 g/mol, MS (E.I.) *m/z* 449 (1%) [M]⁺, 435 (18%) [M – Me]⁺, 392 (100%) [M – CMe₃]⁺.

3.7.3. 1-Bis(difluoro-methyl)silylamino-1,1-di-*tert*-butyl-3,3,3-trimethyl-1,3-disiloxane (**30**)

B.p. 121 °C/10 mbar. Yield: 42%. NMR (CDCl₃): ¹H δ 1.06 SiC(CH₃)₃ (18H), 0.49 F₂SiCH₃ (t, ³J_{HF} = 0.51 Hz, 6H), 0.22 Si(CH₃)₃ (9H); ¹³C δ 28.15 SiC(CH₃)₃, 21.80 SiC(CH₃)₃, 2.84 Si(CH₃)₃, –0.31 F₂SiCH₃ (t, ²J_{CF} = 23.5 Hz), –2.35 F₂SiCH₃ (t, ²J_{CF} = 23.0 Hz); ¹⁹F δ 43.17, 42.33; ²⁹Si δ 9.27 Si(CH₃)₃, –2.98 SiC(CH₃)₃, –32.63 SiF₂ (t/t, ¹J_{SiF} = 279.9 Hz, ³J_{SiF} = 3.3 Hz), –33.66 SiF₂ (t, ¹J_{SiF} = 281.9 Hz). C₁₃H₃₃F₄NOSi₄, 407.74 g/mol, MS (E.I.) *m/z* 392 (18%) [M – Me]⁺, 350 (100%) [M – CMe₃]⁺.

Table 3

Compound	25	26	28
Identification code			
Empirical formula	C ₄₁ H ₈₀ F ₂ LiNO ₄ Si ₃	C ₄₄ H ₁₀₄ F ₂ N ₆ O ₂ Si ₆	C ₂₃ H ₃₇ F ₄ NOSi ₄
Formula weight	780.27	955.87	531.90
<i>T</i> (K)	200(2)	200(2)	150(2)
<i>λ</i> (pm)	71.073	71.073	71.073
Crystal system	Monoclinic	Triclinic	Triclinic
Space group	<i>P</i> 2(1)/ <i>c</i>	<i>P</i> $\bar{1}$	<i>P</i> $\bar{1}$
Unit cell dimensions			
<i>a</i> (pm)	2180.3(10)	970.51(19)	1004.5(2)
<i>b</i> (pm)	1235.5(3)	1196.8(2)	1089.7(2)
<i>c</i> (pm)	1860.3(4)	1337.4(3)	1272.4(3)
α (°)	90	9.68(3)	90.62(3)
β (°)	102.65(3)	72.17(3)	97.71(3)
γ (°)	90	75.07(3)	97.91(3)
<i>V</i> (nm ³)	4.89(1)	1.4243(5)	1.3664(5)
<i>Z</i>	4	1	2
<i>D</i> _{calc} (Mg/m ³)	1.060	1.114	1.293
Absorption coefficient (mm ^{−1})	0.140	0.191	0.261
<i>F</i> (000)	1712	528	564
Crystal size (mm ³)	1.00 × 0.80 × 0.60	1.00 × 0.80 × 0.40	0.70 × 0.60 × 0.60
θ Range for data collection (°)	3.55–22.53	3.54–22.52	3.56–25.03
Index ranges	−23 ≤ <i>h</i> ≤ 23, −13 ≤ <i>k</i> ≤ 12, −20 ≤ <i>l</i> ≤ 17	−9 ≤ <i>h</i> ≤ 10, −12 ≤ <i>k</i> ≤ 12, −14 ≤ <i>l</i> ≤ 14	−11 ≤ <i>h</i> ≤ 11, −12 ≤ <i>k</i> ≤ 12, −15 ≤ <i>l</i> ≤ 15
Reflections collected	7427	5837	8342
Independent reflections (<i>R</i> _{int})	5232 (0.0648)	3688 (0.0947)	4780 (0.0532)
Completeness	to $\theta = 22.53^\circ$, 81.6%	to $\theta = 22.52^\circ$, 98.4%	to $\theta = 25.03^\circ$, 99.6%
Maximum and minimum transmission	0.9209 and 0.8730	0.9276 and 0.8322	0.8589 and 0.8382
Refinement method	Full-matrix least-squares on <i>F</i> ²	Full-matrix least-squares on <i>F</i> ²	Full-matrix least-squares on <i>F</i> ²
Data/restraints/parameters	5232/0/487	3688/0/287	4780/0/307
Goodness-of-fit on <i>F</i> ²	1.033	1.021	1.055
Final <i>R</i> indices [<i>I</i> > 2 σ (<i>I</i>)]	<i>R</i> ₁ = 0.0925, <i>wR</i> ₂ = 0.2494	<i>R</i> ₁ = 0.0459, <i>wR</i> ₂ = 0.1321	<i>R</i> ₁ = 0.0589, <i>wR</i> ₂ = 0.1554
<i>R</i> indices (all data)	<i>R</i> ₁ = 0.1090, <i>wR</i> ₂ = 0.2714	<i>R</i> ₁ = 0.0478, <i>wR</i> ₂ = 0.1351	<i>R</i> ₁ = 0.0667, <i>wR</i> ₂ = 0.1637
Largest difference peak and hole (e Å ^{−3})	1.362 and −0.602	0.431 and −0.322	0.977 and −0.578

3.8. X-ray crystal structure determinations of 4, 8, 11, 17, 20, 21, 22, 23, 24, 25, 26 and 28

X-ray data collection and refinement. Crystal data are summarized in Tables 1–3. Data were collected on a Stoe AED2 four-circle diffractometer. Monochromated Mo K α radiation ($\lambda = 71.073$) was used. The structures were solved by direct methods [16]. All non-hydrogen atoms were refined anisotropically [17]. The structures were refined against F^2 . For the hydrogen atoms bonded to carbon the riding model was used. The hydrogen atoms bonded to nitrogen or oxygen were refined with distance restraints.

3.9. Computational details

Quantum chemical (density functional, DFT) calculations have been carried out to shed more light on the different isomers and various substitution effects. Though the calculations were performed for isolated molecules in the gas phase, the results can well be compared with our experiments that were conducted in aprotic, non-polar solvents.

All structures reported in this work were fully optimized employing the three-parameter hybrid method of Becke, B3LYP [18,19], first in conjunction with the 6-31G(d) basis set. The optimized geometry was further refined using the 6-311+G(2d,p) basis that contains diffuse functions and additional polarization functions at the hydrogens to guarantee an appropriate description of the anionic centers and the loose bonding situation in the saddle point structures. Hessian matrices at all stationary points on the PES were calculated to verify their nature. The geometries of the first order saddle points (“transition states”) were identified using the intrinsic reaction coordinate (IRC) method [20,21]. All computations were carried out using the program package GAUSSIAN-98 [22].

4. Summary

That aminosilanol and their alkaline salts react with halosilanes to aminosiloxanes has been proven by experiments and rationalized by calculations. In further reactions, the second silyl group may be bonded to the nitrogen or oxygen atoms. Normally, the aminosiloxanes form alkaline ions, silylamino-silanolates. This includes a 1.3-silyl group migration from oxygen to the nitrogen atom. The isomerisation reaction can be prevented sterically by bulky groups, and electronically by difluorosilyl groups, and amido-1.3-disiloxanes are formed. LiF-elimination from lithium salts of fluoro-functional amino-1.3-disiloxanes leads to four- or eight-membered (SiNSiO) ring systems. Silyl group

migration does not occur in reactions of 1-silylamino-1.3-disiloxanes with lithium organyls. Always, the lithium-1-silylamido-1.3-disiloxane is formed. For that reason, no isomerisation occurs and a third silyl group will be bonded to the nitrogen atom.

The chemical behavior of aminosilanol is proven by experiments, crystal structure determinations, and quantum chemical calculations.

Acknowledgements

We are grateful to the Deutsche Forschungsgemeinschaft and the Fonds der Chemischen Industrie for support of this work. The calculations were carried out at the Gesellschaft für wissenschaftliche Datenverarbeitung Göttingen (GWDG).

References

- [1] S. Kliem, U. Klingebiel, S. Schmatz, *J. Organomet. Chem.* 686 (2003) 16.
- [2] O. Graalman, U. Klingebiel, W. Clegg, M. Haase, G.M. Sheldrick, *Angew. Chem.* 96 (1984) 904; *Angew. Chem., Int. Ed. Engl.* 23 (1984) 891.
- [3] O. Graalman, U. Klingebiel, *J. Organomet. Chem.* 275 (1984) C1.
- [4] C. Reiche, S. Kliem, U. Klingebiel, M. Noltemeyer, C. Voit, R. Herbst-Irmer, S. Schmatz, *J. Organomet. Chem.* 667 (2003) 24.
- [5] L.H. Sommer, J. Tyler, *J. Am. Chem. Soc.* 76 (1954) 1030.
- [6] P.D. Lickiss, *Adv. Inorg. Chem.* 42 (1995) 147; P.D. Lickiss, in: Z. Rappoport, Y. Apeloig (Eds.), *The Chemistry of Organic Silicon Compounds*, vol. 3, Wiley, New York, 2001, p. 695.
- [7] K. Ruhlandt-Senge, R.A. Bartlett, M.M. Olmstead, P.P. Power, *Angew. Chem.* 105 (1993) 459; *Angew. Chem., Int. Ed. Engl.* 32 (1993) 425.
- [8] R. Murugavel, M. Bhattadarjee, H.W. Roesky, *Appl. Organomet. Chem.* 13 (1999) 227.
- [9] D. Schmidt-Bäse, U. Klingebiel, *J. Organomet. Chem.* 364 (1989) 313.
- [10] K. Dippel, U. Klingebiel, G.M. Sheldrick, D. Stalke, *Chem. Ber.* 120 (1987) 611.
- [11] U. Klingebiel, M. Noltemeyer, *Eur. J. Inorg. Chem.* (2001) 1889.
- [12] S. Kliem, U. Klingebiel, in: H.A. Oye (Ed.), *Silicon for the Chemical Industry VI*, Trondheim, Norway, 2002, p. 139.
- [13] R. Wolfgramm, T. Müller, U. Klingebiel, *Organometallics* 17 (1998) 3222.
- [14] S. Schmatz, F. Diedrich, C. Ebker, U. Klingebiel, *Eur. J. Inorg. Chem.* 2002 (2002) 876.
- [15] S. Schmatz, C. Ebker, T. Labahn, H. Stoll, U. Klingebiel, *Organometallics* 22 (2003) 490.
- [16] G.M. Sheldrick, *Acta Crystallogr., Sect. A* 46 (1990) 476.
- [17] G.M. Sheldrick, *SHELXL-97*, University of Göttingen, Göttingen, Germany, 1997.
- [18] A.D. Becke, *J. Chem. Phys.* 98 (1993) 5648.
- [19] C. Lee, W. Yang, R.G. Parr, *Phys. Rev. B* 37 (1988) 785.
- [20] C. Gonzalez, H.B. Schlegel, *J. Chem. Phys.* 90 (1989) 2154.
- [21] C. Gonzalez, H.B. Schlegel, *J. Phys. Chem.* 94 (1990) 5523.
- [22] M.J. Frisch, G.W. Trucks, H.B. Schlegel, G.E. Scuseria, M.A. Robb, J.R. Cheeseman, V.G. Zakrzewski, J.A. Montgomery, R.E. Stratmann, J.C. Burant, S. Dapprich, J.M. Millam, A.D.

Daniels, K.N. Kudin, M.C. Strain, O. Farkas, J. Tomasi, V. Barone, M. Cossi, R. Cammi, B. Mennucci, C. Pomelli, C. Adamo, S. Clifford, J. Ochterski, G.A. Petersson, P.Y. Ayala, Q. Cui, K. Morokuma, D.K. Malick, A.D. Rabuck, K. Raghavachari, J.B. Foresman, J. Cioslowski, J.V. Ortiz, A.G. Baboul, B.B. Stefanov, G. Liu, A. Liashenko, P. Piskorz, I.

Komaromi, R. Gomberts, R.L. Martin, D.J. Fox, T. Keith, Al-M.A. Laham, C.Y. Peng, A. Nanayakkara, C. Gonzales, M. Challacombe, P.M.W. Gill, B. Johnson, W. Chen, M.W. Wong, J.L. Andres, C. Gonzales, Head-M. Gordon, E.S. Replogle, J.A. Pople, GAUSSIAN-98. Revision A.7, Gaussian, Inc., Pittsburgh, PA, 1998.